

2009

Study of mercury transformation with chlorinated species under homogeneous and heterogeneous conditions

Bhargavi Busireddy
University of Dayton

Follow this and additional works at: https://ecommons.udayton.edu/graduate_theses

Recommended Citation

Busireddy, Bhargavi, "Study of mercury transformation with chlorinated species under homogeneous and heterogeneous conditions" (2009). *Graduate Theses and Dissertations*. 13.
https://ecommons.udayton.edu/graduate_theses/13

This Thesis is brought to you for free and open access by the Theses and Dissertations at eCommons. It has been accepted for inclusion in Graduate Theses and Dissertations by an authorized administrator of eCommons. For more information, please contact mschlangen1@udayton.edu, ecommons@udayton.edu.

Study of Mercury Transformation with Chlorinated Species
under Homogeneous and Heterogeneous Conditions

Thesis

Submitted to

The School of Engineering of the

UNIVERSITY OF DAYTON

in Partial Fulfillment of the Requirements for

The Degree

Master of Science in Materials Engineering

by

Bhargavi Busireddy


UNIVERSITY OF DAYTON


Dayton, Ohio

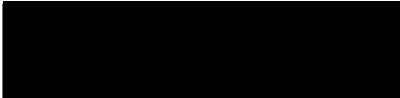
May, 2009

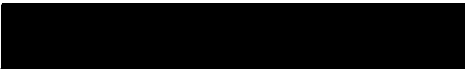
STUDY OF MERCURY TRANSFORMATION WITH CHLORINATED SPECIES
UNDER HOMOGENEOUS AND HETEROGENEOUS CONDITIONS


APPROVED BY:

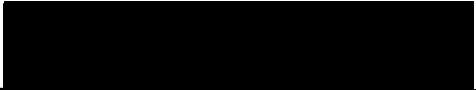

Philip H. Taylor, Ph.D.
Advisory Committee Chairman
Professor of Electro-Optics, Group Leader
and Distinguished Research Scientist, UDRI
Environmental Engineering Group


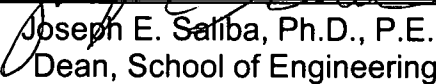

Takahiro Yamada, Ph.D.
Research Advisor
Senior Research Scientist, UDRI
Environmental Engineering
Group


Paul T. Murray, Ph.D.
Committee Member,
Professor, Materials Engineering


Donald A. Klosterman, Ph.D.
Committee Member,
Assistant Professor,
Chemical & Materials Engineering


Daniel Eylon, D.Sc.
Academic Advisor
Professor and Director, Materials Engineering


Malcolm W. Daniels, Ph.D.
Associate Dean,
School of Engineering



Joseph E. Saliba, Ph.D., P.E.
Dean, School of Engineering

ABSTRACT

STUDY OF MERCURY TRANSFORMATION WITH CHLORINATED SPECIES UNDER HOMOGENEOUS AND HETEROGENEOUS CONDITIONS

Name: Bhargavi Busireddy
University of Dayton

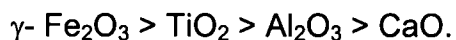
Research Advisor: Dr. Takahiro Yamada

Academic Advisor: Dr. Daniel Eylon

Mercury (Hg) transformation under homogeneous (gas-phase oxidation reactions primarily involving chlorine species in flue gases) and heterogeneous (gas-surface oxidation reactions involving surface enhanced Hg oxidation in the presence of flue gases) environments were investigated. Gas phase experiments were performed in the presence of chlorine sources such as Cl_2 and HCl . A large body of literature studies indicates that during combustion in coal-fired power plants coal mineral matter components play a major role in Hg transformation. Surface activity of these components with respect to Hg adsorption and overall Hg removal were evaluated using a laboratory-scale, fixed bed flow reactor where initial Hg concentration, temperature, residence time, gas composition, and the metal oxide surface were carefully controlled. The metal oxides of interest were $\gamma\text{-Fe}_2\text{O}_3$, TiO_2 , Al_2O_3 , and CaO . These catalytic materials were immobilized between quartz wool in a quartz flow reactor.

Homogeneous experiments with different gas compositions, different chlorine sources (HCl or Cl₂), and gas-phase residence times of 1 and 2 sec showed no measurable difference in Hg oxidation except at 100°C. Hg removal (oxidation) efficiencies ranged from 2 to 15%.

Heterogeneous studies in the presence of metal oxides (with Cl₂ and HCl as the chlorine source) indicated that γ -iron oxide showed the highest Hg removal efficiency at 1 sec residence time, compared to other metal oxides under the same experimental conditions. However, the data were highly scattered and occasionally showed inconsistency. A reduction in the surface activity of γ -iron oxide due to aging may have been responsible for the inconsistency in some of the results. TiO₂, used in the presence of Cl₂ at 100°C, resulted in a 60% Hg removal efficiency which decreased with increasing temperature. TiO₂ used in the presence of HCl resulted in a 55% Hg removal efficiency at 400°C. Al₂O₃ and CaO were ineffective with regard to Hg oxidation in the presence of Cl₂ or HCl compared to γ -iron oxide and TiO₂. Adsorption and overall Hg removal efficiencies showed the following trend (in descending order of effectiveness):



ACKNOWLEDGEMENTS

I would like to thank my research advisor, Dr. Takahiro Yamada, for providing this opportunity to carry out my research (through funding from the Ohio Coal Development Office) and for his continual support in helping me understand the practical aspects of the research and for answering my many questions. I would like to thank Dr. Phil Taylor for his support and guidance and for obtaining additional funding from the Ohio Board of Regents. I would like to thank my academic advisor, Dr. Daniel Eylon, for encouraging me to work for the environmental group of UDRI. My special thanks to Dr. Terry Murray and Dr. Donald Klosterman for being part of my committee.

I gratefully acknowledge the Ohio Coal Development Office and the Ohio Board of Regents for providing financial assistance for this project.

TABLE OF CONTENTS

ABSTRACT	iii
ACKNOWLEDGEMENTS	v
LIST OF FIGURES	viii
LIST OF TABLES	xi
I INTRODUCTION AND STATEMENT OF THE PROBLEM	1
II LITERATURE REVIEW	6
Gas phase Hg speciation	9
Effect of O ₂ on Hg	12
Heterogeneous Hg Speciation	12
Effect of Hg Speciation with Fe ₂ O ₃	13
Effect of Hg Speciation with Al ₂ O ₃	14
Effect of Hg Speciation with TiO ₂	15
Effect of Hg Speciation with CaO	15
III OBJECTIVES	18
IV EXPERIMENTAL APPROACH	19
Fixed bed reactor	21
Temperature-controlled furnace	21
AA Hg analyzer	23
Gas composition and residence time	24
Introduction of Hg and chlorine sources	25
Surface materials	27
Characteristics of the surface materials	27
Experimental procedure	29
Hg adsorption	29
Overall Hg removal efficiency	30

Calculations	30
Hg concentration.....	30
Hg gas flow rate	31
Flow rates of Cl ₂ and HCl sources	32
Flow rates of N ₂ , CO ₂ , and O ₂ at 100°C and 1 sec	32
V RESULTS AND DISCUSSION	35
Homogenous gas phase oxidation studies	35
Heterogeneous Hg Reaction studies	39
Effect of TiO ₂ in Hg removal	40
Effect of Al ₂ O ₃ in Hg removal	47
Effect of CaO in Hg removal	53
Effect of γ-Fe ₂ O ₃ in Hg removal.....	59
VI CONCLUSIONS	72
VII RECOMMENDATION FOR FUTURE WORK	73
VIII REFERENCES	74

LIST OF FIGURES

Figure 2.1: Mercury species distribution in coal fired utility boiler flue gas.....	8
Figure 2.2: Cl-atom recycle during homogeneous Hg oxidation	10
Figure 4.1: Experimental setup	20
Figure 4.2: Reactor wall temperature profile	23
Figure 4.3: Hg in ice bath.....	26
Figure 4.4: Schematic of Reactor mounted with quartz wool and surface material	28
Figure 5.1: Hg overall removal efficiency vs. temperature after 1 ppm Cl ₂ injection gas phase 1 sec	36
Figure 5.2: Hg overall removal efficiency vs. temperature after 1 ppm Cl ₂ injection gas phase 2 sec.....	37
Figure 5.3: Hg overall removal efficiency vs. temperature after 100 ppm HCl injection gas phase 1 sec.....	38
Figure 5.4: Hg overall removal efficiency vs. temperature after 100 ppm HCl injection gas phase 2 sec.....	39
Figure 5.5: Hg removal efficiency as a function of temperature with 0.564 g of TiO ₂ , R.T. 1 sec.....	41
Figure 5.6: Hg removal efficiency as a function of temperature with 0.564 g of TiO ₂ R.T. 2 sec.....	42

Figure 5.7: Overall Hg removal efficiency as a function of temperature after 1 ppm Cl ₂ injection with 0.564 g TiO ₂ , R.T. 1 sec.....	43
Figure 5.8: Overall Hg removal efficiency as a function of temperature after 1 ppm Cl ₂ injection with 0.564 g TiO ₂ , R.T. 2 sec.....	44
Figure 5.9: Overall Hg removal efficiency as a function of temperature after 100 ppm HCl injection with 0.564 g of TiO ₂ , R.T. 1 sec.....	45
Figure 5.10: Overall Hg removal efficiency as a function of temperature after 100 ppm HCl injection with 0.564 g of TiO ₂ , R.T. 2 sec.....	46
Figure 5.11: Hg removal efficiency as a function of temperature with 0.560 g of Al ₂ O ₃ , R.T. 1 sec.....	47
Figure 5.12: Hg removal efficiency as a function of temperature with 0.560 g of Al ₂ O ₃ , R.T. 2 sec.....	48
Figure 5.13: Overall Hg removal efficiency as a function of temperature after 1 ppm Cl ₂ injection with 0.560 g of Al ₂ O ₃ , R.T. 1 sec.....	49
Figure 5.14: Overall Hg removal efficiency as a function of temperature after 1 ppm Cl ₂ injection with 0.560 g of Al ₂ O ₃ , R.T. 2 sec.....	50
Figure 5.15: Overall Hg removal efficiency as a function of temperature after 100 ppm HCl injection with 0.560 g of Al ₂ O ₃ , R.T. 1 sec.....	51
Figure 5.16: Overall Hg removal efficiency as a function of temperature after 100 ppm HCl injection with 0.560 g of Al ₂ O ₃ , R.T. 2 sec.....	52
Figure 5.17: Hg removal efficiency as a function of temperature with 0.5374 g of CaO, R.T. 1 sec.....	53
Figure 5.18: Hg removal efficiency as a function of temperature with 0.5374 g of CaO, R.T. 2 sec.....	54
Figure 5.19: Overall Hg removal efficiency as a function of temperature after 1 ppm Cl ₂ injection with 0.5374 g CaO, R.T. 1 sec.....	55
Figure 5.20: Overall Hg removal efficiency as a function of temperature after 1 ppm Cl ₂ injection with 0.5374 g CaO, R.T. 2 sec.....	56
Figure 5.21: Overall Hg removal efficiency as a function of temperature after 100 ppm HCl injection with 0.5374 g of CaO, R.T. 1 sec.....	57

Figure 5.22: Overall Hg removal efficiency as a function of temperature after 100 ppm HCl injection with 0.5374 g of CaO, Residence time 2 sec	58
Figure 5.23: Hg removal efficiency as a function of temperature with 0.564 g of Fe ₂ O ₃ , R.T. 1 sec	60
Figure 5.24: Hg removal efficiency as a function of temperature with 0.564 g of Fe ₂ O ₃ , R.T. 2 sec	61
Figure 5.25: Overall Hg removal efficiency as a function of temperature after 1 ppm Cl ₂ injection with 0.564 g Fe ₂ O ₃ , R.T. 1 sec	63
Figure 5.26: Overall Hg removal efficiency as a function of temperature after 1 ppm Cl ₂ injection with 0.564 g Fe ₂ O ₃ , R.T. 2 sec	64
Figure 5.27: Overall Hg removal efficiency as a function of temperature after 100 ppm HCl injection with 0.564 g Fe ₂ O ₃ , R.T. 1 sec.....	65
Figure 5.28: Overall Hg removal efficiency as a function of temperature after 100 ppm HCl injection with 0.564 g Fe ₂ O ₃ , R.T. 2 sec.....	66
Figure 5.29: Hg removal efficiency as a function of temperature after 1 ppm Cl ₂ injection in presence of N ₂ gas with combination of all catalysts and Gas phase: Residence time 1 sec	68
Figure 5.30: Hg removal efficiency as a function of temperature after 1 ppm Cl ₂ injection in presence of N ₂ gas with combination of all catalysts and Gas phase: Residence time 2 sec	69
Figure 5.31: Hg removal efficiency as a function of temperature after 100 ppm HCl injection in presence of N ₂ gas with combination of all catalysts and Gas phase: Residence time 1 sec.....	70
Figure 5.32: Hg removal efficiency as a function of temperature after 100 ppm HCl injection in presence of N ₂ gas with combination of all catalysts and Gas phase: Residence time 2 sec.....	71

LIST OF TABLES

Table 4.1: Specifications of furnace	22
Table 4.2: Specifications of MFCs used in the experiment	25
Table 4.3: Properties of metal surfaces	27
Table 4.4: Characteristics of metal surfaces	28
Table 4.5: Experimental conditions at 100°C	33
Table 4.6: Experimental conditions at 200°C	33
Table 4.7: Experimental conditions at 300°C	34
Table 4.8: Experimental conditions at 400°C	34

CHAPTER I

INTRODUCTION

Mercury (Hg), commonly referred to as quicksilver (during ancient times), is a heavy, odorless metal belonging to group (IIB) of the Periodic Table. Unlike the other IIB group elements, Hg exhibits two oxidation states: mercurous, Hg^+ and mercuric, Hg^{2+} . Hg metal is widely distributed in nature; however, it is usually found in low concentrations. The occurrence of Hg ranges from 50 ppb (parts per billion) in terrestrial abundance to 100 ppb in soils, and 10 to 20,000 ppb in rocks.¹

The properties of Hg include uniform volume expansion over its entire liquid range, as well as high surface tension; i.e., inability to wet and cling to make glass. These properties make Hg essential for barometers, manometers, thermometers and many other measuring devices. Because of its low electrical resistivity, Hg is rated as one of the best electric conductors among the metals. Hg also has the ability to form alloys known as amalgams.

Mercury occurs in different chemical forms in the environment, which vary depending on the source type and other factors. There are three primary categories of Hg: elemental, organic and inorganic compounds. Elemental Hg, a shiny and silver-white metal which is liquid at room temperature, is considered as the main form of mercury that is released into air as vapor. Hg has a vapor pressure of 0.5426 Pascal (Pa) at 30°C², and exhibits a significant vapor-phase concentration at ambient temperatures. Elemental Hg is considered to be soluble in lipids and nitric acid, and is insoluble in hydrochloric acid and water. Inorganic mercury enters the air from mining ore deposits, burning coal and waste.³

During the industrial age, Hg levels in the environment have been increasing. Global release of Hg into the environment can be either natural or anthropogenic. Natural Hg sources are considered to be mainly from volcanoes and volatilization of Hg from water, soils, flora and fauna.⁴ Anthropogenic releases result from the combustion of coal, mining and processing of metals, chlor-alkali (mercury cell) production, and releases from landfills.

Hg has many applications and end uses in various fields. Some of them are batteries, pigments, catalysts, explosives, special paper coating, pharmaceuticals, electrolytic preparation of chlorine and caustic soda, automobile convenience switches, dental amalgam, fluorescent lamps and lab/medical use including thermometers and thermostats.¹ Because of the

concern for mercuric toxicity from environmental pollution and occupational exposure, the demand for mercury has decreased in documented applications.⁴

Human and animal exposure to Hg from the general environment occurs mainly by inhalation and ingestion of terrestrial and aquatic food chain items. Hg in the air eventually settles into water or on land, where it can be washed into water. The toxic effects of mercury and mercury compounds are known; the toxicity to the central nervous system is more prominent after exposure to mercury vapor than to divalent mercury. Short-term exposure to mercury vapor may produce symptoms within a few hours. These symptoms include weakness, chills, metallic taste, nausea, vomiting, diarrhea, labored breathing, cough, and a feeling of tightness in the chest. Chronic exposure to Hg vapor produces an insidious form of toxicity that is manifested by neurological effects and is referred to as asthenic vegetative syndrome. The syndrome is characterized by tremors, psychological depression, irritability, excessive shyness, insomnia, emotional instability, forgetfulness, confusion, and uncontrolled blushing.⁵

In order to decrease the amount of anthropogenic Hg released in the United States, the United States Environmental Protection Agency (US-EPA) has limited both the use and disposal of mercury. The Clean Air Act of 1970 (amended in 1990) provides a regulatory means to reduce mercury emissions and limit the use of Hg. In December 1997, the US-EPA published a report on mercury emissions which identified Hg as an environmental hazard and

expressed the need for further research related to the reduction of mercury. The report estimated that coal combustion produces about 72 tons of Hg emissions.⁶ A February 1998 US-EPA published report stated that electrical utilities are the largest sources of Hg emissions into air. The report estimated that U.S. coal burning power plants emit approximately 50 tons of elemental mercury.⁵

Coal-fired utility boilers are presently the largest significant source of mercury emissions in the U.S. The US-EPA Information Collection Request (EPA-ICR) for coal burning utilities indicated there were 70 tons of mercury in the 900 million tons of coal burned in U.S. power plants during 1999. Based on the EPA-ICR, the estimated total Hg emissions from coal-fired plants ranged from 40 to 52 tons. On average, 40% of Hg entering a coal-fired power plant is captured and 60% is emitted. On March 15, 2005, the US-EPA decided that Hg emissions should be reduced to 31.3 tons in 2010, 27.9 tons in 2015, and 24.3 tons in 2020.⁷

Hg emissions continue to be a significant air pollution problem globally. During Feb 20, 2009 meeting the governing council of the United States Environmental Program (UNEP) decided to reduce mercury pollution, with more than 140 countries agreeing in principle to a global treaty to control Hg.⁸

To support pending US-EPA regulations, Hg emissions for individual plants were measured based on type of coal and emission control equipment.

The various types of emission control equipment examined included selective catalytic reduction (SCR), electrostatic precipitators (ESPs), and flue gas desulfurizers (FGD). The results indicated that the percent of Hg emission varied widely (from as low as 40% to nearly 100% removal). Cleaning of coal is considered one relatively simple Hg control technology based on the form of Hg present in coal. Removal of 0 to 60% Hg is reported as a physical washing method, whereas advanced cleaning methods and hydrothermal treatment offer slightly higher removal efficiency of not more than 70%.⁹

Knowledge of the chemical and physical transformations of Hg in coal-fired power plants is necessary to reduce the emissions of Hg in the environment. Hg can be catalyzed by the metals present in coal in the presence of NO_x or HCl. An analysis conducted by the Electric Power Research Institute (EPRI), indicated that high levels of coal chlorine content correlated with an increase in Hg capture and a decrease in percentage of Hg⁰, while higher levels of coal sulfur correlated with a reduction in Hg capture. The oxidized form of Hg can be easily removed by acid gas scrubbers due to its solubility in aqueous solutions. From coal combustion in the coal-fired power plant, Hg in its oxidized form is thought to be HgCl₂. Compared to elemental Hg, HgCl₂ is slightly less volatile at stack temperatures and at lower ambient temperatures. The factors that control the separation of mercury between its elemental and oxidized states are thought to be important in understanding Hg emissions.

CHAPTER II

LITERATURE REVIEW

Hg emissions from coal-fired power plants are highly variable and difficult to effectively control as the flue gas concentrations are one million times lower than other pollutants of concern. In December 2000, the US-EPA recommended further research to attempt to develop control technologies.

Coal contains Hg in trace amounts on the order of 0.1 ppm. Coal burning combustors are a major source of anthropogenic Hg emissions because during the combustion process Hg is volatilized and converted to elemental Hg.¹⁰ The chemical transformation of Hg in the different zones of a power plant plays a key role in determining its fate.

Sorbents have been considered a means to capture Hg in the combustion zone. To aid in Hg capture, various studies have examined many different sorbents such as fly ash, activated carbon, metal oxides, etc. Among all sorbents, metal oxides were the most effective because of their resistivity to temperature.¹¹ Dunham's study with fixed bed interactions between Hg and fly

ash concluded that fly ashes have the capability of oxidizing Hg, but relatively few of them were also capable of capturing mercury. For example, among fly ash constituents, magnetite has the effective capability of oxidizing elemental Hg; as the percent of magnetite increases in fly ash, oxidation also increases. The surface area and the nature of surface material play a major role in understanding the oxidation and adsorption of Hg.⁹ Sondreal predicted that iron oxides are capable of oxidizing Hg, and that oxidation improved in the presence of HCl. Sondreal studied the oxidation of Hg with maghemite, which is an intermediate state of iron oxide. The mechanism involved between HCl and maghemite was not understood, but it has been assumed that either catalytic activity of chlorine or surface activity of maghemite might enhance the oxidation of Hg.¹²

Figure 2.1 describes the transformation of Hg in a coal-fired utility boiler, with a boiler temperature of 1500°C. At this temperature, Hg vaporizes and becomes stable in elemental Hg form. When elemental Hg passes through the post-combustion zone, it reacts with acid gases at low temperatures in the presence of fly ash constituents, and transforms into oxidized form.

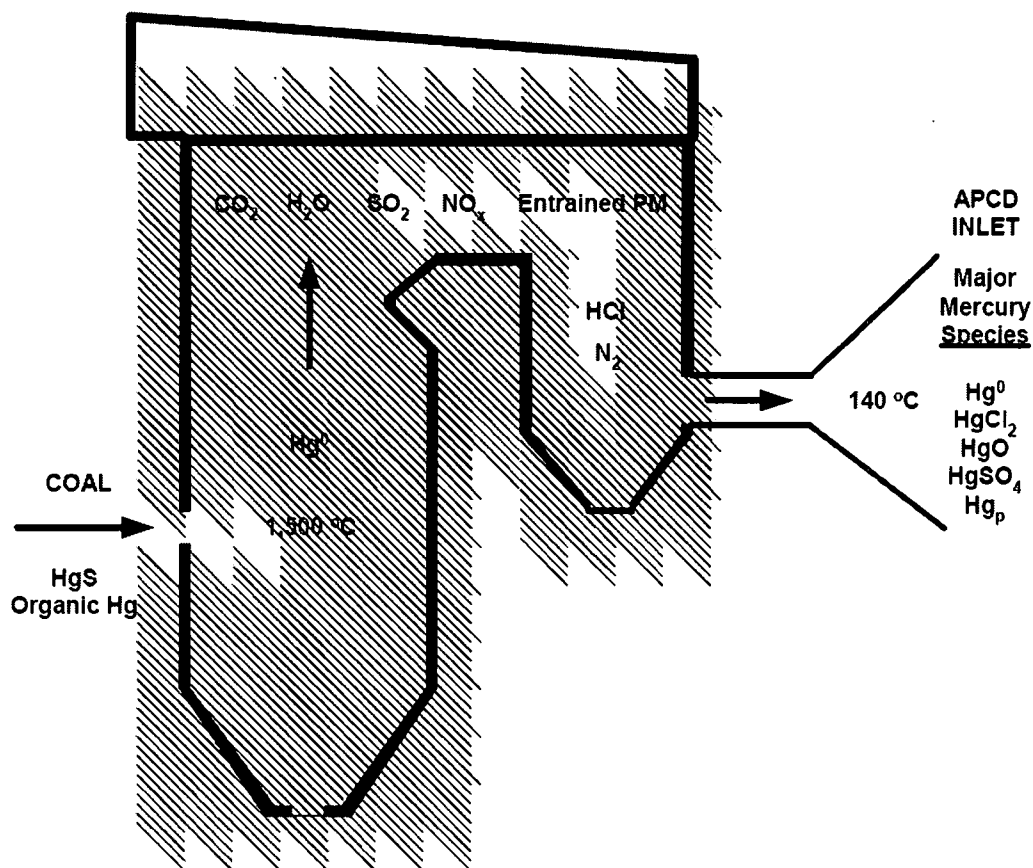


Figure 2.1: Mercury species distribution in coal fired utility boiler flue gas¹³

Understanding the transformation of Hg during the coal combustion process is an important part of controlling mercury emissions because there are different forms of mercury in flue gases, formed either by oxidation or by reduction reactions. Homogenous and heterogeneous reactions help to understand the behavior of Hg and Hg flue gas chemistry in the combustion zone,^{14,9} depending on the coal characteristics, flue gas chemistry and combustion conditions. Chlorine sources are believed to affect Hg speciation in flue gas through homogeneous and heterogeneous reactions. Using reactive

chlorine sources such as atomic chlorine (Cl) and molecular chlorine (Cl₂), homogeneous elemental Hg-chlorine reactions occur effectively when compared to HCl, as HCl in its reduction state cannot oxidize elemental Hg directly.¹⁵ According to Niksa, heterogeneous Hg and chlorine reactions follow two mechanisms; the first is the bonding of Hg directly by a chlorinated site on solid surface. The second mechanism is the indirect Hg oxidation reaction that occurs by transforming of atomic chlorine (Cl) to molecular (Cl₂).¹⁶

Gas phase Hg speciation:

Transformation of Hg is mainly influenced by temperature, flue gas composition, and residence time.¹⁷ Gas phase oxidation reactions are mainly considered to involve potential chlorine sources in the flue gas. Atomic chlorine in flue gas is considered to be the dominant sources in oxidation of elemental Hg.^(18,19) Kinetic studies have reported large rate constants for both k_1 and k_2 ($k_2 = 1.95 \pm 1.05 \times 10^{13} \text{ cm}^3/\text{mol-s}$) for the following reactions of Hg with Cl:



These studies found that the higher the chlorine atom concentration, the higher will be the Hg oxidation in the gas phase.

Chlorine improved the vaporization of Hg, and Hg reacted with flue gases at higher temperatures to form HgCl_2 (g), HgO (g), and Hg^0 (g). Among these three forms of Hg, HgCl_2 (g) is dominant at temperatures below 450°C .¹⁷ Figure 2.2 explains the sub-mechanism for the Cl atom recycle involving in Hg oxidation proposed by Niksa. The diagram shows that the partial oxidation between Hg^0 and Cl atom forms HgCl , producing HgCl_2 by further reaction with Cl_2 .²⁰

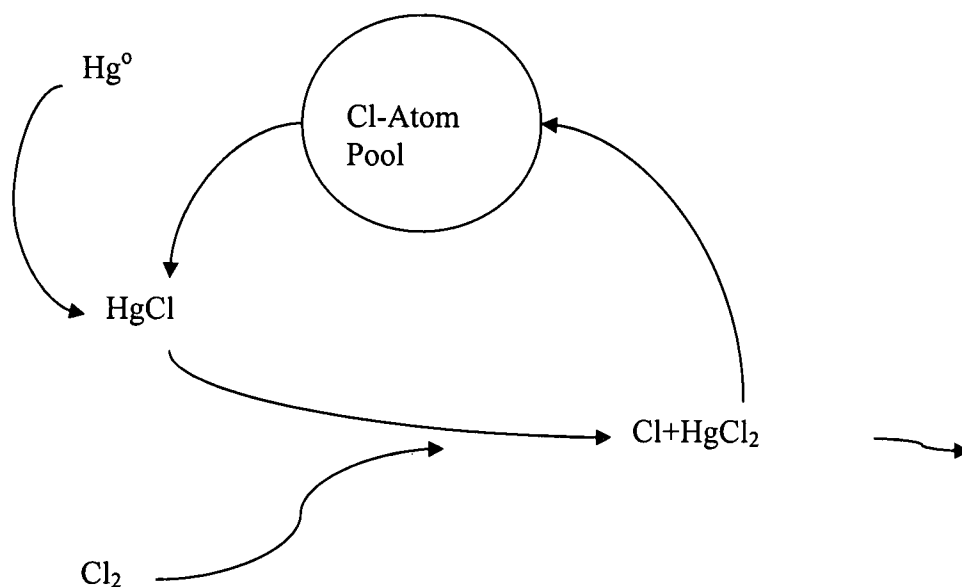
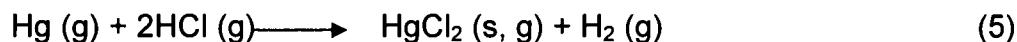
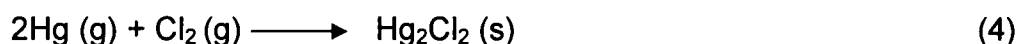
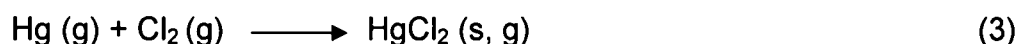
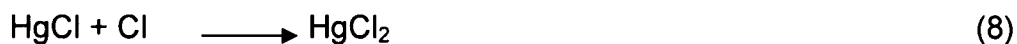


Figure 2.2: Cl-atom recycle during homogeneous Hg oxidation²⁰

Hall proposed reactions for elemental Hg and acid gases such as Cl_2 and HCl and determined a rate constant from kinetic data.²¹ The data indicated that the reaction of Hg (g) with Cl_2 is greater than the reaction of Hg (g) with HCl by about three orders of magnitude. Rate constants were presented as $4.1 \times 10^{-16} \text{ cm}^3/\text{molecule-sec}$ for reactions with $\text{Hg} + \text{Cl}_2$, and $< 1.0 \times 10^{-19} \text{ cm}^3/\text{molecule-sec}$ for reactions with $\text{Hg} + \text{HCl}$ at temperatures ranging from 20 to 900°C .



Kramlich²² proposed sub-mechanisms involving Hg, Cl₂ and HCl. In this report, he suggested that $\text{Hg} + \text{Cl} \longrightarrow \text{HgCl}$ is the fastest reaction to occur during Hg oxidation at room temperature. The rate constants for reactions (6), (7) and (8) were presented as $k = 1.95 \pm 1.05 \times 10^{13} \text{ cm}^3/\text{mol}\cdot\text{s}$. This work also presented several additional pathways involving oxidation of HgCl to HgCl₂:



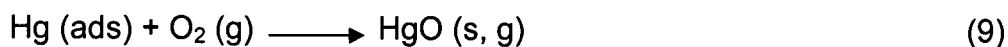
Kramlich and Niksa proposed the same kind of reaction pathways for the oxidation of Hg with Cl.^{22, 20} Both authors discussed the mechanism, but Niksa demonstrated the oxidation of Hg with atomic chlorine using the chlorine atom recycle mechanism detailed in Figure 2.2.²⁰ This explains the partial oxidation of Hg and Cl to form HgCl and the further formation of HgCl₂ with Cl₂.

The gas phase study by Ghorishi indicated that the oxidation of elemental mercury is slow in the presence of HCl, but effective at temperatures greater than

700°C for concentrations of HCl in the range 100-200 ppm.²³ The studies of Hall and Schager showed that the reaction between elemental mercury and HCl was temperature sensitive and proceeded faster at temperature > 500°C. HCl was shown to be a very good oxidizing agent, especially in the presence of metal oxides. In this process, it follows the deacon reaction mechanism and converts into chlorine, which is also a very good oxidizing agent.^{24,21} It can be concluded that the reaction for Hg and Cl, Hg and Cl₂ is fast compared to the reaction for Hg and HCl. While the reaction for Hg and HCl can be effective at temperatures greater than 500°C and HgCl₂, it is considered to be the dominant product at temperatures less than 450°C.

Effect of O₂ with Hg:

Hall indicated an increase in the reaction rate of Hg and O₂ with increases in temperature until it reaches the decomposition temperature.²¹



Galbreath reported that adsorbed Hg⁰ or O₂ on the surface could lead to heterogeneous reactions, resulting in HgO (g).²⁵



Heterogeneous Hg Speciation:

In the combustion zone, chemical reactions proceed at high temperatures rather than under post-combustion conditions. It is believed that Hg transformations are controlled by heterogeneous reactions which occur in the

post-combustion zone. Gas-phase reactions alone are not sufficient to describe the Hg transformation in flue gas. Metallic oxides of fly ash are found to promote Hg oxidation, especially in the presence of HCl. Hg capture increased when flue gas temperature was reduced to below 400°C.²⁶

HgO (g) formation involves heterogeneous reactions of Hg⁰ (ads) with O₂ adsorbed on a catalyst surface. Initially, mercury oxidation studies were conducted in the presence of fly ash, which was shown to enhance the Hg oxidation reactions in the post-combustion zone. This study provided strong evidence that catalytic surfaces play an important role in explaining the surface catalytic mechanism in the post-combustion zone. It is very important to explain the role of fly ash constituents, such as Fe₂O₃, Al₂O₃, TiO₂, and CaO in the transformation of Hg to HgO and HgCl₂ under the influence of flue gas compositions.⁹

Effect of Hg Speciation with Fe₂O₃:

As mentioned earlier, metallic oxides showed to be more effective than activated carbon in enhancing Hg oxidation. Iron oxide, one of the metallic constituents of fly ash, tested to be a better catalyst in improving the oxidation of Hg. Zhuang study demonstrated that iron oxide promoted Hg oxidation in the presence of HCl.¹⁵ This has also been shown by Ghorishi, who conducted Hg speciation experiments using a fixed bed reactor with HCl concentration ranging

from 100-200 ppm in the presence of metal oxides, such as iron oxide, alumina, silica, calcium oxide and copper oxide.²³

α -Iron oxide was ineffective when injected into fly ash in the presence of HCl, but α -Iron oxide and γ -iron oxide were effective in enhancing the Hg oxidation in the presence of HCl and NO_x . In his study, Galbreath concluded that γ -iron oxide readily captures Hg^0 . The availability of Hg^{2+} , HCl and γ -iron oxide in excess in the Blacksville coal combustion flue gas suggested that γ -iron oxide catalyzes Hg^{2+} formation in the presence of HCl and elemental Hg. The experimental conditions maintained at 150°C in the fabric filter containing 65 g/m² of γ -iron oxide with combustion flue gases flowing through fabric filter resulted in 30% of elemental Hg being converted to Hg^{2+} and Hg (p) with 100 ppmv of HCl injection. The addition of more HCl and γ -iron oxide did not have any effect on elemental mercury oxidation.²⁷

Effect of Hg Speciation with Al_2O_3 :

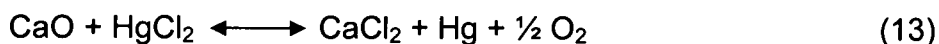
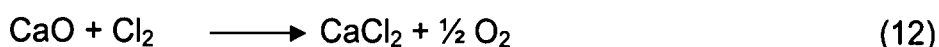
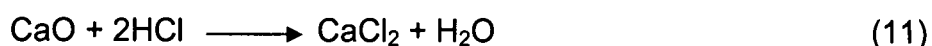
Hg transformations using an aluminum oxide catalyst show no significant differences. The various studies gave the same results, proving that aluminum oxide is inactive in the capture of mercury. Mercury speciation in the presence of alumina using 100 ppm of HCl concentration in a fixed bed reactor was ineffective. The results obtained by Galbreath demonstrated that using 50-100 ppm of HCl for speciation of mercury in the presence of alumina were also ineffective.^{23, 25, 15}

Effect of Hg Speciation with TiO₂:

Galbreath's results demonstrated the inability of titanium dioxide to promote Hg oxidation.²⁵ The reasons for this inability were not clear, but Galbreath proved that either the chemically complex flue gas might catalytically affect TiO₂ or the catalyst itself is not a good oxidizing agent. The experiments were conducted in a cylinder containing working standard grade HCl (g) (10290 ± 510 ppmv in N₂) with a permeation tube used as source of Hg⁰, which was connected to an inline mercury analyzer at flue gas temperatures 970, 620 and 250°C.

Effect of Hg Speciation with CaO:

Calcium oxide was found to be sensitive to the formation of Hg and flue gas composition in an experiment performed to find the role of calcium in the presence of HCl for Hg oxidation and adsorption.²⁸ Calcium oxide was not effective in capturing Hg. This study also showed that calcium-rich adsorbents adsorb oxidized Hg. When acid gases were introduced, the adsorption of acid gases prevailed and oxidation decreased. Investigations by Hocquel explained the role of CaO in the presence of HCl for Hg speciation as a function of temperature. A continuous emission monitor was used for analyzing Hg. CaO played a key role in the transformation of ionic HgCl₂ (g) into Hg⁰ (g). In the combustion process, the reactions were feasible between temperatures of 300 to 600 K.²⁹ According to Hocquel's experiments, the following reactions were possible:



Hocquel concluded that under influence of different temperatures and HCl concentrations, CaO improves the adsorption of Hg.

This research was performed in an effort to systematically study the oxidation and adsorption of Hg using both a gas phase and gas-surface reaction system. From the literature review, it is known that in the combustor the Hg present in coal is converted to gaseous elemental Hg. Elemental Hg is subsequently oxidized in the post-combustion zone, where the temperature is much lower than average temperatures in the combustor.¹⁰ Gas-phase Hg oxidation reactions are mainly those involving different chlorine sources such as Cl_2 or HCl , whereas heterogeneous Hg oxidation reactions also involve various surfaces including metal oxides associated with fly ash generated from the high-temperature transformation of the mineral matter originally present in the coal. In the presence of chlorine and surfaces, Hg oxidation occurs under both homogeneous and heterogeneous oxidation conditions.¹¹ In addition, it has been shown that the heterogeneous oxidation of Hg is influenced by the post-combustion flue gas composition, including constituents such as NO_x , SO_x , O_2 ,

and water vapor. This thesis will focus on the effects of acid gases on the oxidation of Hg in the presence of different metal oxide surfaces.

CHAPTER III

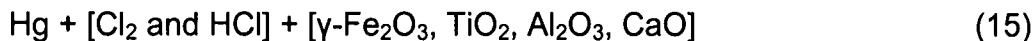
OBJECTIVES

The primary objective of this research was to understand the fundamental reaction mechanism of Hg chlorination in homogeneous and heterogeneous environments in order to elucidate Hg transformation in the power plant post-combustion zone. Homogeneous reactions involve the gas-phase interaction between elemental Hg and chlorine sources such as Cl_2 and HCl . Heterogeneous reactions involve interactions between elemental Hg and chlorine sources in the presence of metal oxides ($\gamma\text{-Fe}_2\text{O}_3$, TiO_2 , Al_2O_3 , and CaO). The experiments were performed at constant initial Hg concentration as a function of residence time (1 and 2 sec), temperature (100-400°C) and flue gas compositions (N_2 , N_2+CO_2 , $\text{N}_2+\text{CO}_2+\text{O}_2$). The following reactions were studied:

Homogeneous (gas-phase) reaction:



Heterogeneous (gas-surface) reaction:



CHAPTER IV

EXPERIMENTAL APPROACH

The experiments performed for this study were conducted with an assembly of instruments and a data acquisition procedure with flow reactor apparatus, trace level Hg analyzer, and data reduction method for homogeneous and heterogeneous chlorination of elemental mercury. A separate fused silica quartz tube was used for each experiment, and carrier gas with varied compositions was passed through the reactor which contained surface materials, where mercury chlorination reactions were performed.

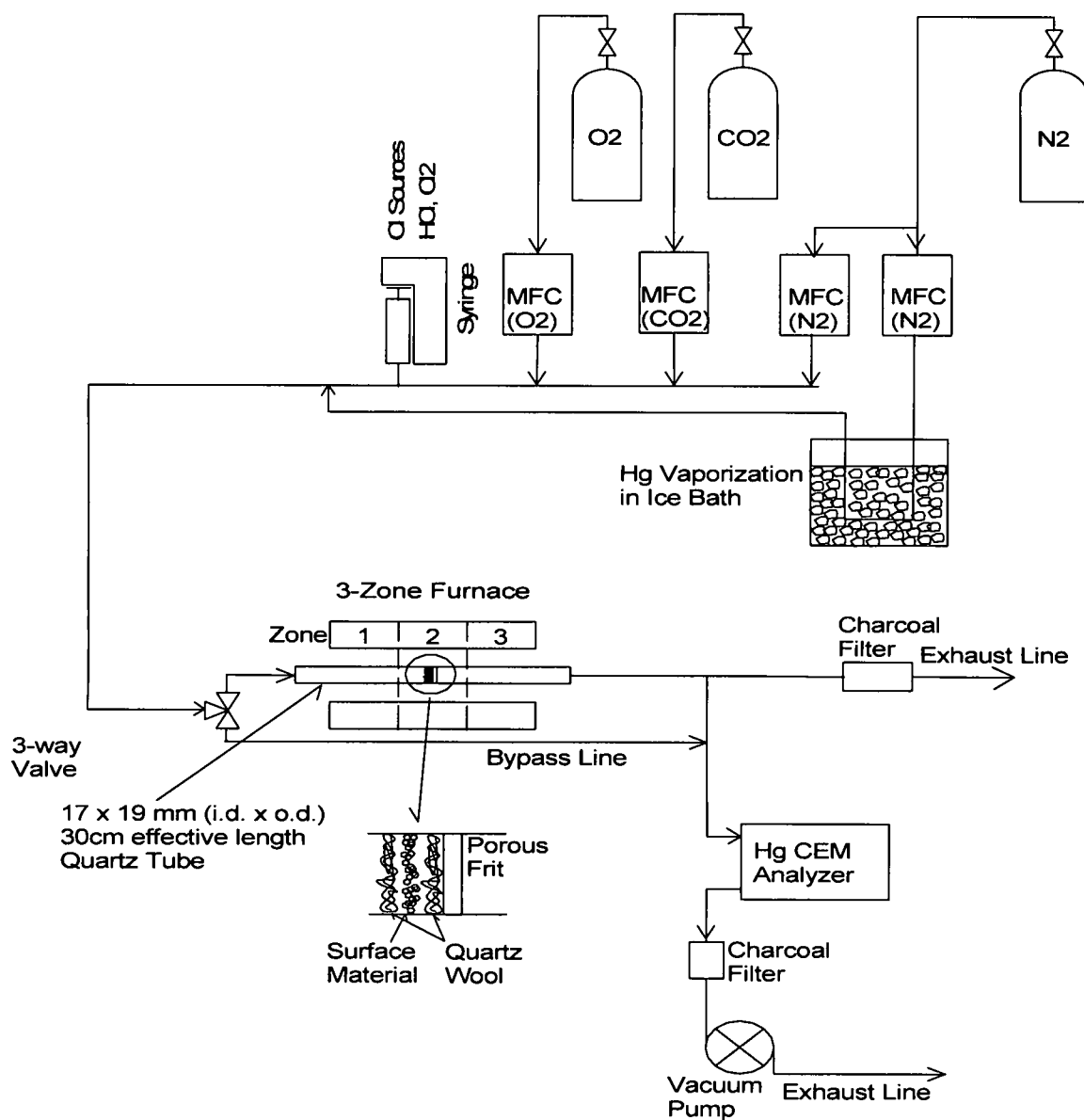


Figure 4.1 Schematic of Experimental Setup

Fixed Bed Reactor:

The fused silica flow reactor (17 i.d. x 19 mm o.d. x 70 cm length) purchased from Quartz Scientific, Inc was used for the heterogeneous reactions. The pure metal oxides were placed in the center of the reactor and immobilized with porous quartz filter discs (Quartz Scientific, Inc., porosity extra coarse (00) microns, nominal pore size 200-300 microns) and quartz wool (Technical Glass Products, Inc.). The fixed bed reactor was housed in a three-zone temperature controlled furnace. This particular silica flow reactor has a low coefficient of thermal expansion, which imparts a high resistance to thermal shock.

Temperature Controlled Furnace:

The reactor temperature was controlled using a three-zone temperature furnace (TZF 12/38/400, Carbolite, Inc.) with a specific feature that provided linear temperature uniformity. The maximum operating temperature of the furnace was 1200°C. Temperature sensors, such as thermocouples, were used for axial thermal uniformity. These sensors were located in the protected position between the outside of the work tube and heating element, allowing the full work tube diameter to be used. This model used three resistance wire heating elements wound around the integral ceramic work tube. The uniformity of the heat in the furnace was achieved using the three control system, which in turn balanced the power of the heating elements. Table 4.1 describes the

specifications of the furnace such as maximum temperature limit, diameter of the reactor, and heat length of the reactor in the furnace.

Table 4.1: Specifications of furnace

Maximum temperature	1200 °C
Inside diameter of fixed element tube	38 mm
Heat length	400 mm

The temperature profile was determined by performing experiments with Argon inert gas passing through the furnace and by varying the temperature inside the reactor from 100 to 400°C.³⁰ These experiments were performed by a previous UD investigator³⁰ as shown in the Figure 4.2. Figure 4.2 shows that temperature is uniformly distributed in the high temperature zone. The furnace used by the previous investigator was also used in this study. Since the calibrations were done previously, recalibration was not seemed necessary.

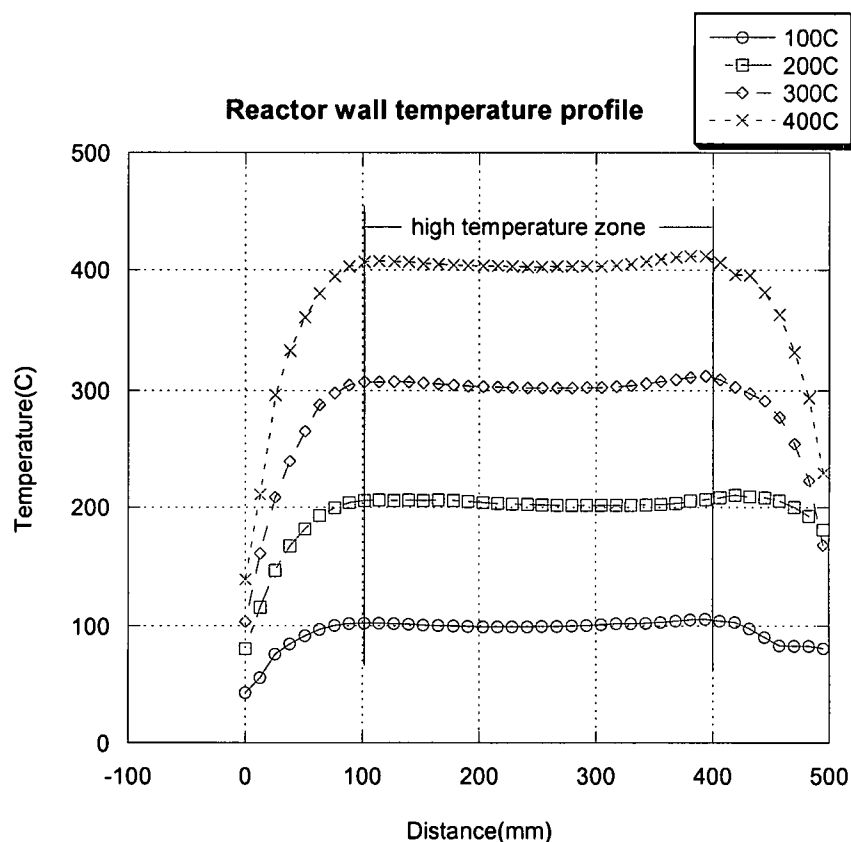


Figure 4.2: Reactor wall temperature profile³⁰

Atomic Absorption Hg Analyzer:

The elemental Hg was measured with an in-line RA-915+ AA Hg Analyzer (Ohio Lumex). The RA-915+ mercury analyzer is a portable multifunctional atomic absorption spectrometer with Zeeman background correction, which eliminates the effect caused by interfering impurities. It is the only high sensitivity and high selectivity instrument that does not require gold amalgam pre-concentration and subsequent regeneration steps, which enables the user to conduct real-time monitoring. The detection limits for elemental Hg in ambient air using this detector are 2 ng/m³ with the multi-photocell and 500 ng/m³ with the single photocell. The Hg analyzer is shown in Figure 4.1.

Gas Composition and Residence Time:

Nitrogen was used as a main carrier gas in the experiments. In order to replicate the typical flue gas compositions in a typical coal-fired power plant, N_2 , O_2 , and CO_2 gases were used. All three gas flows were controlled by digital mass flow controllers (MFC) (Porter Instrument Company, Inc.). Compared to manual flow controllers, these MFCs provide a more accurate and stable flow, and easier flow control. Table 4.2 shows the specification of the MFCs. The gas compositions used for Hg oxidation studies were N_2 , $N_2 + CO_2$, $N_2 + CO_2 + O_2$. In order to replicate the approximate residence times in the post-combustion zones of full-scale systems, residence times of 1 and 2 sec were maintained by varying the flow rates of gases at different temperatures. Hg adsorption and oxidation behaviors were studied as a function of temperature, gas-phase residence time and gas composition.

Table 4.2: Specifications of MFCs used in experiment

MFC Characteristics	Gas			
	N_2	N_2	CO_2	O_2
Model Number	201-DKASVCAA	201-DKASVCAA	201-DKASBCAA	201-DKASVCAA
Flow rate Max.	2000 sccm	1000 sccm	500 sccm	100 sccm
Inlet Pressure (P1) Max.	50 psig	50 psig	50 psig	50 psig
Outlet Pressure (P2) Max.	14.2 psi	14.2 psi	14.2 psi	14.2 psi

Introduction of Hg and Chlorine Sources:

Hg concentration maintained in each experiment was $10 \mu\text{g}/\text{m}^3$ (1.2 ppb). The reason for choosing a $10 \mu\text{g}/\text{m}^3$ concentration was that in coal combustion, flue gas Hg generally ranges from 5 to $20 \mu\text{g}/\text{m}^3$.¹¹ As shown in Figure 4.3, Hg was produced with an Hg vaporization/saturation tube. This saturation tube was designed with a U tube containing Hg immobilized between the quartz wool. The entire setup was placed in an ice bath where the temperature was maintained at 0°C with a Hg vapor pressure of $2.51 \times 10^{-4} \text{ Pa}$.³¹ The Hg concentration was controlled by temperature and the ratio of Hg carrier flow to the main carrier flow. The temperature monitor for the mercury was purchased from Omega Engineering Inc. The temperature of the U-tube in the ice bath was measured using a thermocouple with a 1/16 inch diameter and a 12 inch length. The flow controller used for Hg flow was Model VCD1000 (Porter Instrument Co.). In the flow controllers, flow elements were used to control the flow. The flow element used in the model is red anodized with a silver dot with a maximum flow range of 25 cc/min.

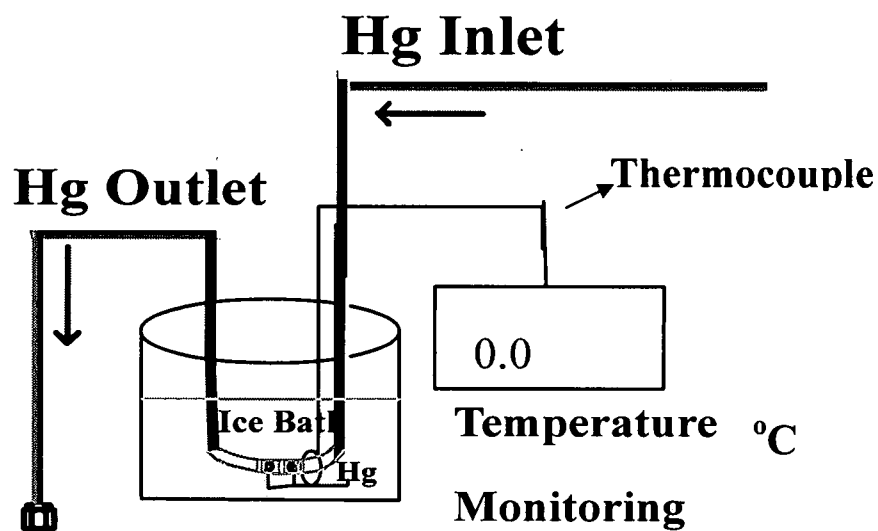


Figure 4.3: Hg in ice bath

The chlorine sources used were HCl and Cl₂ in concentrations of 100 and 1 ppm, respectively. Cl₂ was taken directly from a calibrated compressed gas cylinder using a gas syringe and then introduced into the reactor using a syringe pump (Model No. - 780100V, KD Scientific, Inc.). The flow rate of the chlorine source was maintained based on the carrier gas flow rate, reactor temperature, and residence time. Instead of taking HCl directly from the cylinder, a 1 Liter Tedlar® bag (SKC. Inc., PA) was used. The gas was transferred from the cylinder into the Tedlar bag and the required quantity was taken from the bag using a gas syringe. Using the same syringe pump, HCl was then introduced into the reactor.

Surface Materials:

For the heterogeneous studies, four kinds of metal surfaces were used: $\gamma\text{-Fe}_2\text{O}_3$, TiO_2 , Al_2O_3 , CaO . These metal surfaces were purchased from Sigma Aldrich Chemical, Inc. The properties of $\gamma\text{-Fe}_2\text{O}_3$, TiO_2 , Al_2O_3 , CaO are listed in Table 4.3.

Table 4.3: Properties of metal surfaces

Metal Characteristics	Metal Oxides			
	$\gamma\text{-Fe}_2\text{O}_3$	TiO_2	Al_2O_3	CaO
CAS	1309-37-1	1317-80-2	1344-28-1	1305-78-8
Form	Powder	powder	Powder	Powder
Particle size	$<5\mu\text{m}$	$<5\mu\text{m}$	$10\mu\text{m}$	$<5\mu\text{m}$
Density	---	4.17g/mL at 25°C	-----	3.3g/mL at 25°C
Purity	99+%	99.9+%	99.7%	99.995%

Characteristics of the Surface Materials:

The surface materials were carefully placed in the flow reactor. First, the quartz wool and the particular surface material were measured using a Micro Balance (Model AX26, Mettler Toledo). The quartz reactor was placed vertically and a measured amount of quartz wool was mounted on the frit. The surface material was then transferred onto the quartz wool in such a way that it did not touch the reactor wall. The other end was closed using quartz wool as shown in Figure 4.4. Table 4.4 shows the characteristics of metal surfaces such as surface area and the amount of metal surfaces used in the reactor.

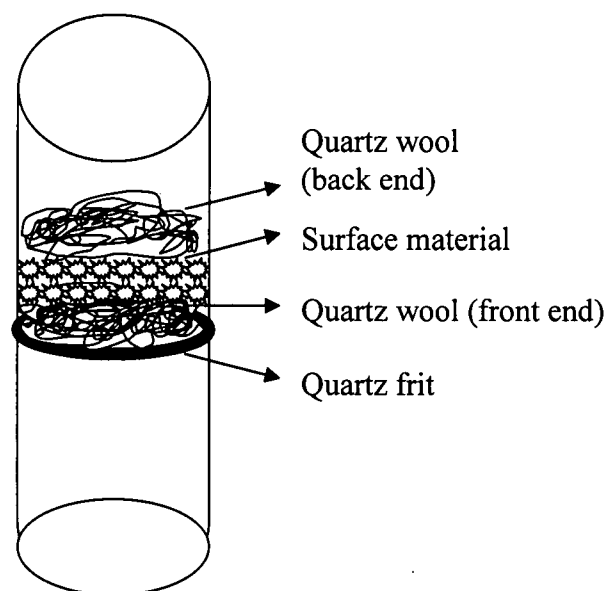


Figure 4.4: Schematic of Reactor mounted with quartz wool and surface material

Table 4.4: Characteristics of metal surfaces

Surfaces	Specific surface area (m ² /g)	Amount (g)	Amount of Quartz wool(g)	
			Front end	Back end
Fe ₂ O ₃	4.86	0.564	0.0289	0.0344
TiO ₂	2.29	0.564	0.0777	0.0380
Al ₂ O ₃	0.81	0.560	0.1033	0.0776
CaO	25.21	0.5374	0.03638	0.0730

Experimental Procedure:

Homogenous and heterogeneous Hg adsorption and oxidation was performed as a function of residence time, gas composition, and temperature. Experimental conditions were maintained at gas-phase residence times of 1 or 2 sec; temperatures of 100, 200, 300 or 400°C; a chlorine source of Cl₂ or HCl, and gas compositions of N₂, N₂+CO₂, or N₂+CO₂+O₂.

For the heterogeneous studies, four different kinds of metal oxides were examined: Fe₂O₃, Al₂O₃, TiO₂, and CaO. In a given experiment, a bypass line was plumbed to the Hg analyzer, which in turn helped calculate the overall oxidation of Hg and the adsorption efficiency of metal oxides. The entire experimental setup is shown in Figure 4.1. Each set of experiments was repeated three times to examine the consistency of the results, and the measurements were averaged.

Hg Adsorption:

In the absence of a chlorine source, Hg adsorption efficiency was calculated at the entrance and exit of the reactor based on the elemental Hg concentration.

$$\text{Hg}^{\circ}_{\text{ads}} = ([\text{Hg}^{\circ}]_{\text{inlet}} - [\text{Hg}^{\circ}]_{\text{outlet}}) / ([\text{Hg}^{\circ}]_{\text{inlet}}) \dots\dots\dots (16)$$

Overall Hg Removal Efficiency:

The overall Hg removal efficiency was calculated based on the measured elemental Hg^0 concentration at the entrance and exit of the reactor in the presence of a chlorine source. The difference was assumed to be either adsorbed or oxidized Hg.

$$\text{Hg}^0 \text{ overall removal} = ([\text{Hg}^0]_{\text{inlet}} - [\text{Hg}^0]_{\text{outletw/Cl}_2}) / ([\text{Hg}^0]_{\text{inlet}}) \dots\dots (17)$$

Calculations:

This section briefly explains the calculations involving to:

- 1) Hg concentration
- 2) Flow rates of gases (N_2 , CO_2 , O_2 , Hg, and Cl_2 and HCl)
- 3) Adsorption and oxidation efficiencies (%)

Hg Concentration:

In order to replicate the post-combustion conditions, the initial concentration of Hg was fixed at $10 \mu\text{g}/\text{m}^3$, which is equivalent to 1.22 ppbv as shown below:

$$10 \mu\text{g of Hg} = 10 \times 10^{-6} \text{ g}$$

$$\text{Mole of Hg} = 10 \times 10^{-6} \text{ g} / 200 \text{ g/mol}$$

From Ideal Gas Law, $V = (nRT) / P$ at 1 atm and 298 K,

$$\begin{aligned} V (\text{L}) &= (10 \times 10^{-6} \text{ g}) / 200 \text{ g/mol} \times 0.0821 (\text{L-atm/mol-K}) \times 298 \text{ K} \\ &= 1.22 \times 10^{-6} \text{ L} / 1000 \text{ L} (1 \text{ m}^3 = 1000 \text{ L}) \end{aligned}$$

$$= 1.22 \text{ ppbv}$$

The experiments were carried out at temperatures of 100°C, 200°C, 300°C, or 400°C for gas-phase residence times of 1 or 2 sec. Example calculations for determining flow rates of mercury, gas constituents and chlorine sources are shown below for conditions of 100°C and 1 sec:

Volume of reactor (1.7 cm i.d., 30 cm length) = 68.1 mL.

At 1 sec residence time, gas flow rate = 4086 mL/min (assuming plug flow distribution in reactor).

Gas Flow Rate at 100°C:

$$\begin{aligned} \text{Volumetric flow rate} &= \frac{\text{Ambient temperature}}{\text{Reactor temperature}} \times \text{flow rate at room temperature} \\ &= \frac{(24+273)}{(100+273)} \times 4086 \\ &= 3253.46 \text{ mL/min} \end{aligned}$$

Hg gas flow rate:

$$\begin{aligned} \text{Concentration of mercury} &= \frac{\text{Vapor pressure}}{\text{Ambient pressure}} \times \frac{\text{Hg carrier gas flow rate}}{\text{Total flow rate}} \\ 1.22 \times 10^{-9} &= \frac{2.23 \times 10^{-4}}{740} \times \frac{\text{Hg carrier gas flow rate}}{3253.5} \end{aligned}$$

$$\text{Hg flow rate} = 13.1 \text{ mL/min}$$

Flow rates of Cl₂ and HCl sources:

$$\text{Concentration of chlorine} = (\text{flow rate of chlorine} \times [1/100]) \times (1/\text{total flow rate})$$

$$1 \times 10^{-6} = (\text{flow rate of chlorine} \times [1/100]) \times (1/3253.5)$$

$$\text{Flow rate of chlorine} = 19.5 \text{ mL/hr}$$

Flow rates of N₂, CO₂, and O₂ at 100°C and 1 sec:

$$\text{Flow rate of CO}_2 = (\text{Volumetric flow rate} \times \text{desired CO}_2 \text{ concentration})/100$$

$$= 3253.5 \times 15/100$$

$$= 488.0 \text{ mL/min.}$$

$$\text{Flow rate of O}_2 = (\text{Volumetric flow rate} \times \text{desired O}_2 \text{ concentration})/100$$

$$= 3253.5 \times 3/100$$

$$= 97.6 \text{ mL/min.}$$

$$\text{Flow rate of N}_2 = \text{Volumetric flow rate} - \text{flow rate of CO}_2 - \text{flow rate of O}_2$$

$$= (3253.5) - (488.0) - (97.6)$$

$$= 2667.9 \text{ mL/min.}$$

Experimental conditions for 100, 200, 300, and 400°C are summarized in Tables 4.5 through 4.8.

Table 4.5: Experimental Conditions at 100°C

Residence time (s)	1	2
Hg gas flow rate (mL/min)	13.14	6.57
Carrier gas flow rate (N ₂) mL/min	2668	1317
Flow rate of O ₂ (mL/min)	98	49
Flow rate of CO ₂ (mL/min)	488	244
Cl ₂ flow rate (mL/hr)	19.5	9.8
HCl flow rate (mL/hr)	19.5	9.8

Table 4.6: Experimental Conditions at 200°C

Residence time (s)	1	2
Hg gas flow rate (mL/min)	10.4	5.2
Carrier gas flow rate (N ₂) mL/min	2077	1039
Flow rate of O ₂ (mL/min)	77	38
Flow rate of CO ₂ (mL/min)	385	192
Cl ₂ flow rate (mL/min)	15.4	7.7
HCl flow rate (mL/min)	15.4	7.7

Table 4.7: Experimental Conditions at 300°C

Residence time (s)	1	2
Hg gas flow rate (mL/min)	8.5	4.3
Carrier gas flow rate (N ₂) mL/min	1715	857
Flow rate of O ₂ (mL/min)	64	32
Flow rate of CO ₂ (mL/min)	318	159
Cl ₂ flow rate (mL/min)	12.7	6.4
HCl flow rate (mL/min)	12.7	6.4

Table 4.8: Experimental Conditions at 400°C

Residence Time (s)	1	2
Hg Gas Flow Rate (mL/min)	7.28	3.64
Carrier Gas Flow Rate (N ₂) mL/min	1460	730
Flow Rate of O ₂ (mL/min)	54	27
Flow Rate of CO ₂ (mL/min)	270	135
Cl ₂ Flow Rate (mL/min)	10.82	5.41
HCl Flow Rate (mL/min)	10.82	5.41

CHAPTER V

RESULTS AND DISCUSSION

Homogenous Gas Phase Oxidation Studies:

Figures 5.1 and 5.2 show the gas phase Hg oxidation after the introduction of 1 ppm of Cl_2 . Equation 17 was used to calculate overall Hg oxidation as mentioned in the experimental approach section. At 1 sec residence, time slight temperature dependence was observed, whereas no temperature dependence was observed at 2 sec residence time. No measurable difference in Hg oxidation was observed between 1 and 2 sec residence time, with the exception 100°C. No significant difference was observed among different gas compositions.

Figures 5.3 and 5.4 show Hg oxidation with 100 ppm of HCl. Similar trends were observed at Hg oxidation with Cl_2 . A small temperature dependence was observed at 1 sec residence time with HCl; no temperature dependence was observed at 2 sec. All of the Hg oxidation efficiencies with Cl_2 and HCl were in the 2 to 15% range.

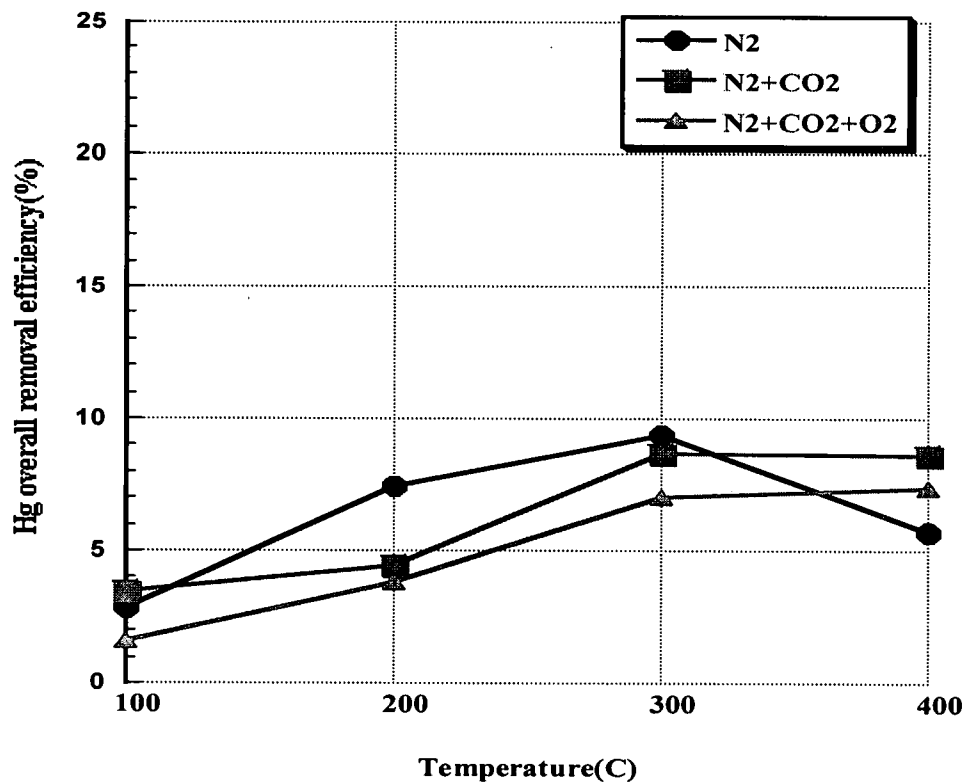


Figure 5.1: Hg Overall removal efficiency vs. temperature after 1 ppm Cl₂ injection, gas phase R.T. = 1 sec

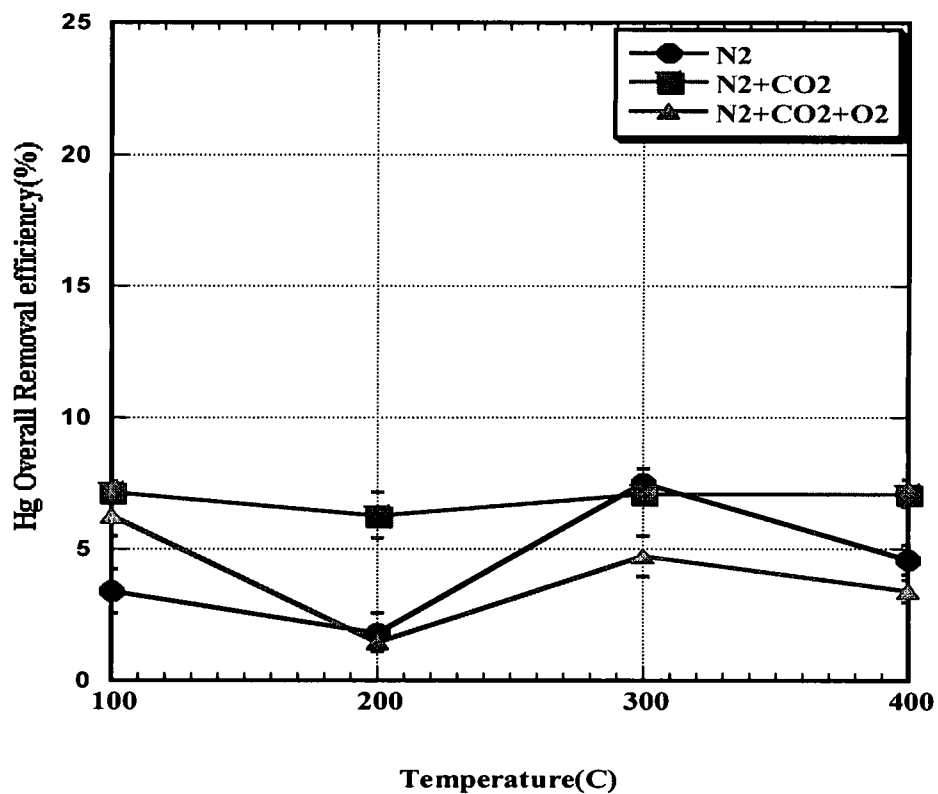


Figure 5.2: Hg overall removal efficiency vs. temperature after 1 ppm Cl₂ injection, gas phase R.T. = 2 sec

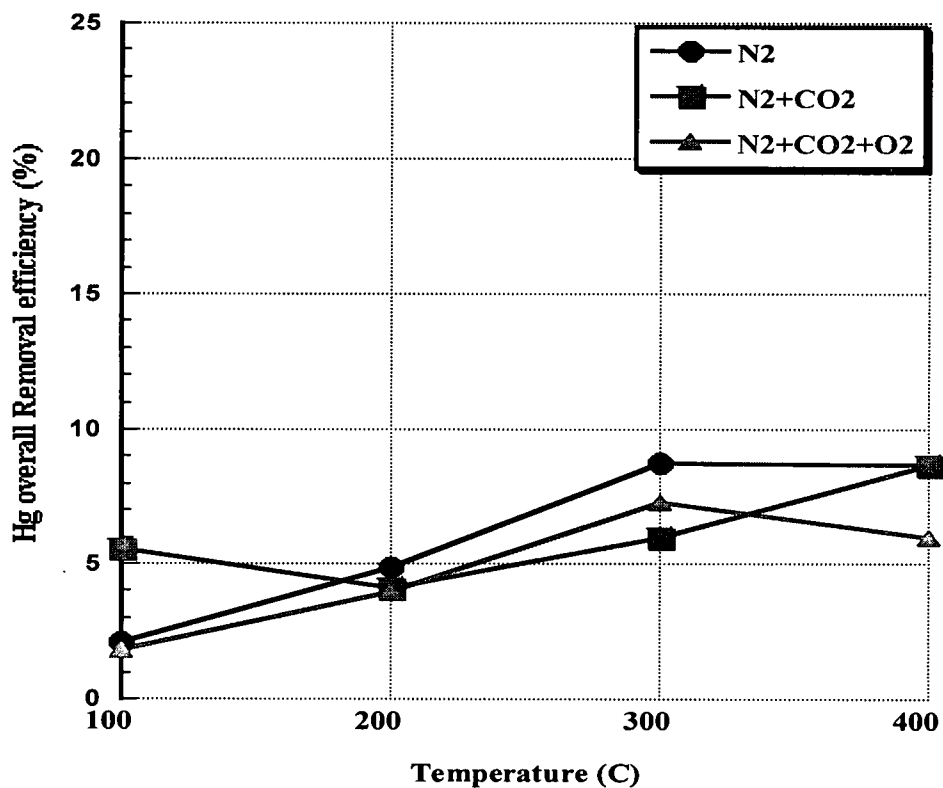


Figure 5.3: Hg overall removal efficiency vs. temperature after 100 ppm HCl injection, gas phase R.T. = 1 sec

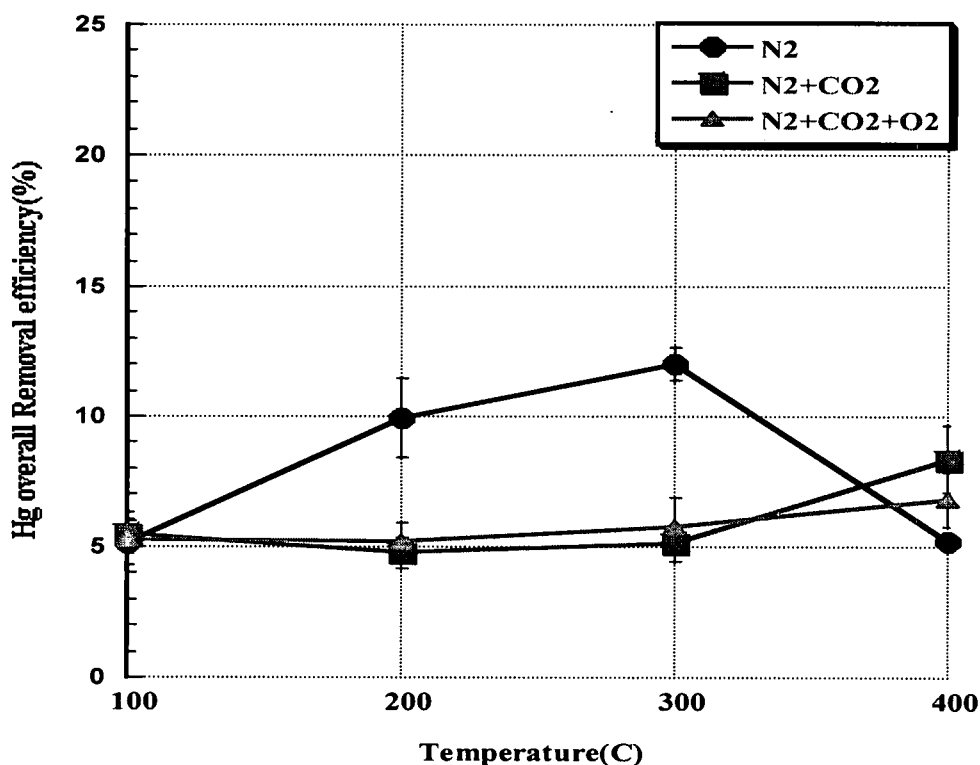


Figure 5.4: Hg overall removal efficiency vs. temperature after 100 ppm HCl injection, gas phase R.T. = 2 sec

Heterogeneous Hg Reaction Studies:

Hg adsorption and overall Hg removal efficiency studies (a combination of adsorption and oxidation) were conducted on the surface of γ -Fe₂O₃, TiO₂, Al₂O₃, CaO. Hg adsorption refers to the Hg loss in the absence of a chlorine source (Cl₂ and HCl) and with the presence of surface material. Overall Hg removal refers to the Hg oxidation in the presence of chlorine sources (Cl₂ and HCl) with or without the presence of a surface material. These catalytic materials were immobilized between quartz wool in the quartz flow reactor. Experiments were

conducted for $\text{Hg} + \text{Cl}_2$ and $\text{Hg} + \text{HCl}$ in order to find mercury adsorption and mercury removal efficiencies using metal oxides. Experimental conditions varied, with temperatures ranging from 100-400°C in 100°C intervals and residence times of 1 and 2 sec with gas compositions N_2 , $\text{N}_2 + \text{CO}_2$, $\text{N}_2 + \text{CO}_2 + \text{O}_2$. The Hg adsorption and overall removal efficiency were calculated based on equations (16) and (17), respectively. Error bars were included in each graph, which were measured from three repeatable experiments conducted for each condition.

Effect of TiO_2 in Hg removal:

Hg adsorption and overall removal efficiencies were plotted as a function of temperature and are shown in Figures 5.5 through 5.16. Figures 5.5 and 5.6 show Hg adsorption efficiencies at 1 and 2 sec residence times. Each line in the graphs represents a different gas composition. In general, adsorption efficiencies were independent of temperature, gas composition, and residence time although adsorption efficiency was slightly higher at the 2 sec residence time for $\text{N}_2 + \text{CO}_2$ and $\text{N}_2 + \text{CO}_2 + \text{O}_2$. All the adsorption efficiencies fall into the 5 to 10% Hg removal range. The TiO_2 surface appears to have a lower adsorption capability than gas phase Hg oxidation.

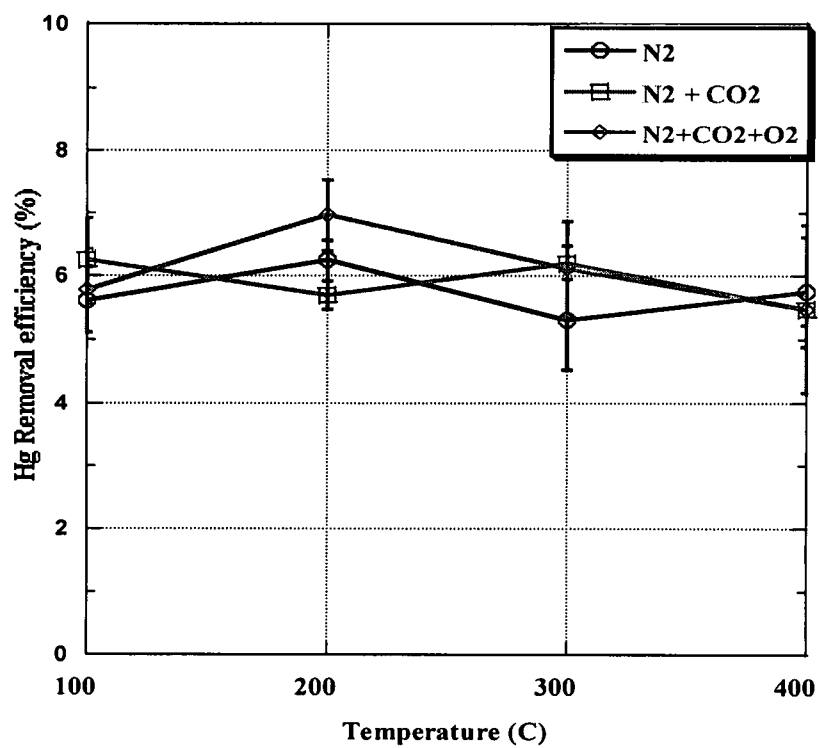


Figure 5.5: Hg removal efficiency as a function of temperature with 0.564 g of TiO₂, R.T. = 1 sec

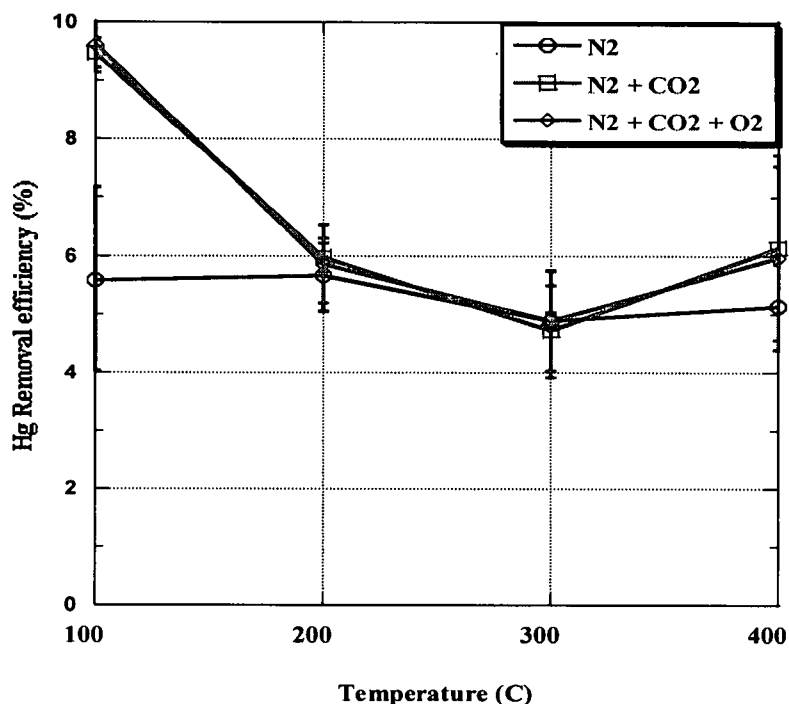


Figure 5.6: Hg removal efficiency as a function of temperature with 0.564 g of TiO₂, R.T. = 2 sec

Figures 5.7 and 5.8 shows the overall Hg removal efficiency with 1 ppm of Cl₂ injection at 1 and 2 sec residence time. The results indicated no significant dependence on residence time and gas composition: however, significant negative temperature dependence was observed. Hg removal efficiencies were highest at 100°C (between 45 and 55%), and the lowest at 400°C (between 10 and 20%). When gas phase oxidation and adsorption efficiencies were taken into account, almost no surface oxidation reaction was observed at 400°C, and approximately 30 to 40% oxidation was observed at 100°C. TiO₂ seems to be a good Hg oxidation catalyst at low temperatures in the presence of Cl₂.

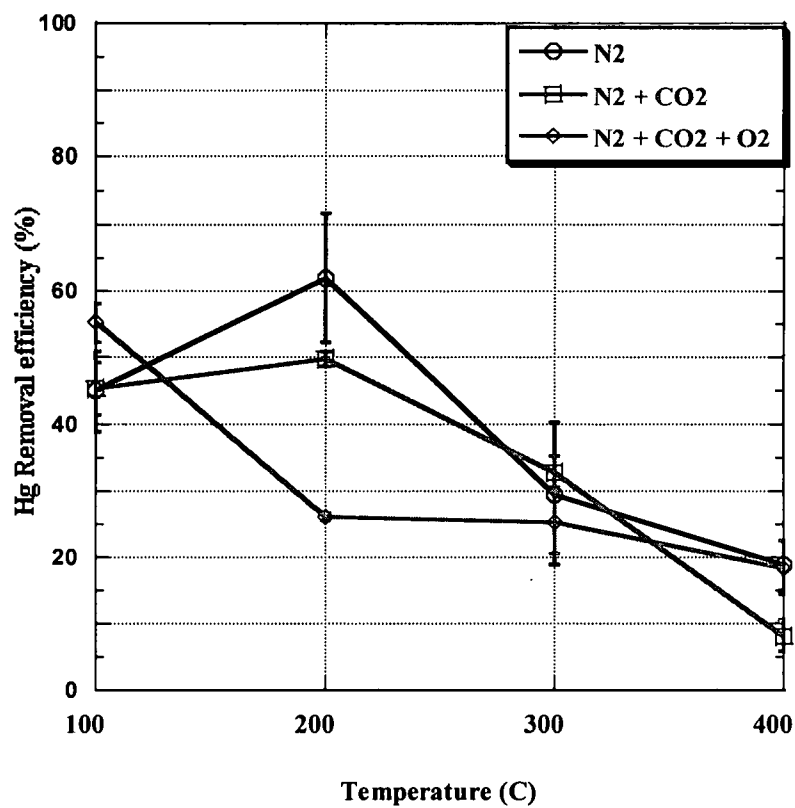


Figure 5.7: Overall Hg removal efficiency as a function of temperature after 1 ppm Cl₂ injection with 0.564 g TiO₂, R.T. = 1 sec

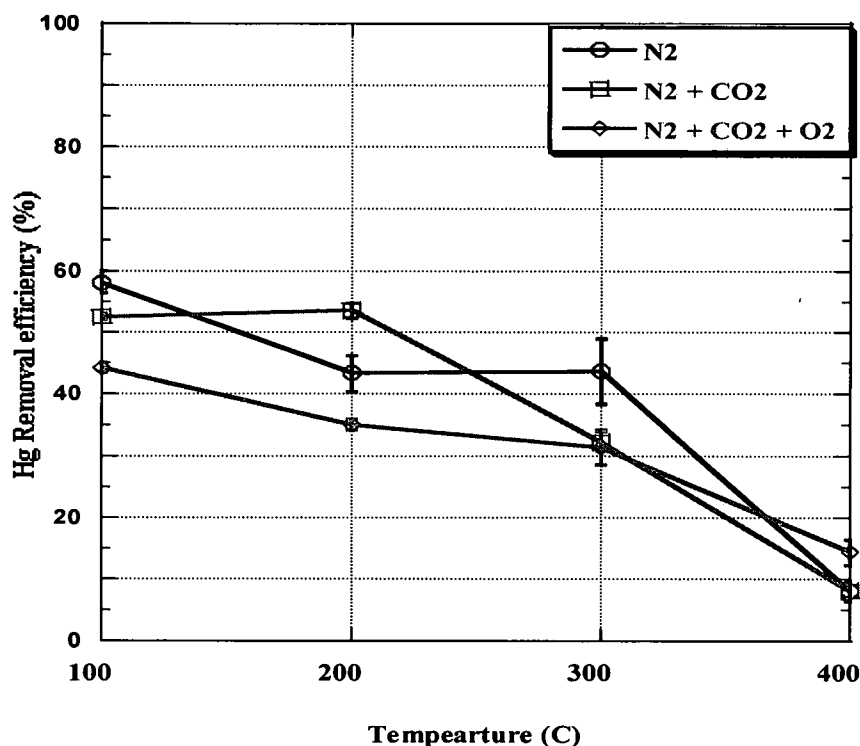


Figure 5.8: Overall Hg removal efficiency as a function of temperature after 1 ppm Cl₂ injection with 0.564 g TiO₂, R.T. = 2 sec

Figures 5.9 and 5.10 represent overall Hg removal efficiency with 100 ppm of HCl injection at 1 and 2 sec residence time. A positive temperature dependence was observed for both 1 and 2 sec residence time experiments, but Hg removal efficiency was larger at 2 sec residence time. Hg removal of 10 to 70% was observed at 400°C depending on the gas composition and residence time. N₂ + CO₂ + O₂ at both residence times showed higher Hg removal, indicating that O₂ might enhance the Hg oxidation in the presence of HCl as shown in the Figures 5.9 and 5.10. TiO₂ could be a good Hg oxidizing catalyst at high temperature with the presence of HCl.

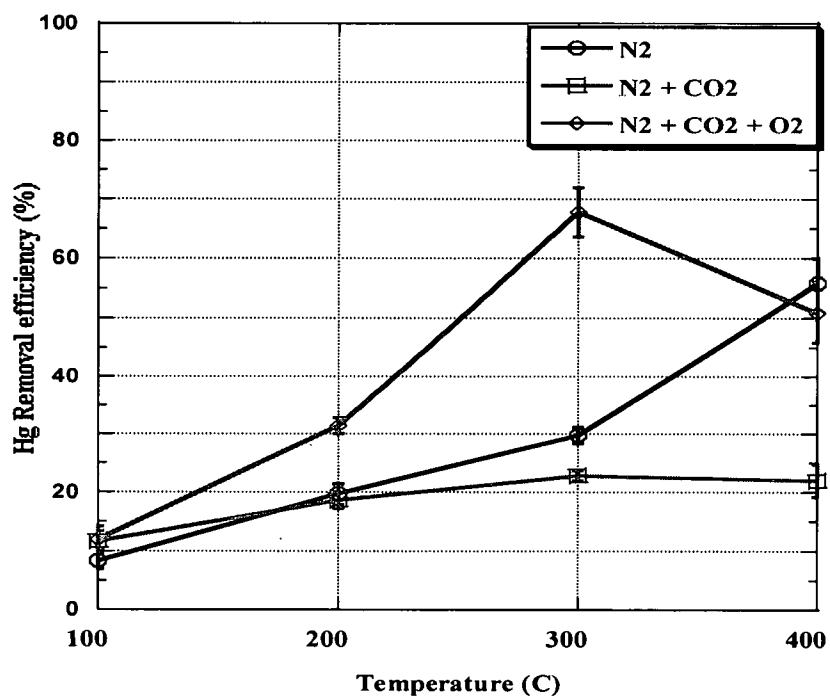


Figure 5.9: Overall Hg removal efficiency as a function of temperature after 100 ppm HCl injection with 0.564 g of TiO_2 , R.T. = 1 sec

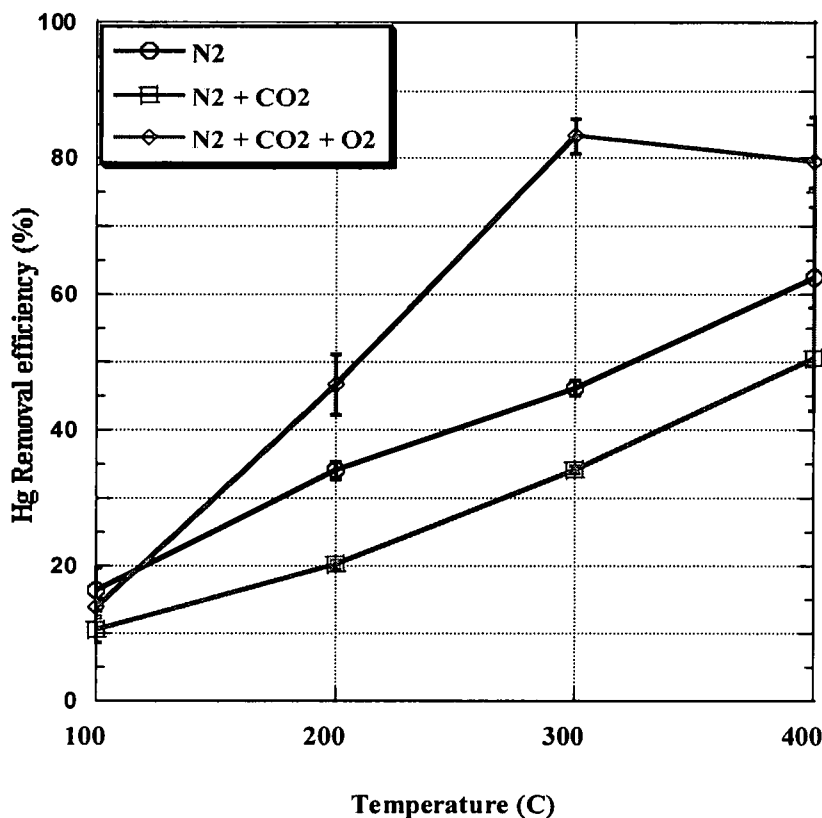


Figure 5.10: Overall Hg removal efficiency as a function of temperature after 100 ppm HCl injection with 0.564 g of TiO₂, R.T. = 2 sec

Galbreath performed measurements of mercury speciation separately in the presence of oxygen and nitrogen by injecting 10 µg/m³ of elemental mercury. Experiments were performed in the presence of the TiO₂ catalyst. The results showed that the catalyst was inactive in the transformation of Hg⁰ to Hg²⁺.³² The current study was the first to examine TiO₂ reactivity in the presence of Cl₂ and HCl, and showed that TiO₂ played an important role in the oxidation of Hg with the presence of Cl₂ at low temperatures up to 200°C. At higher temperatures, TiO₂ played an important role in the presence of HCl.

Effect of Al_2O_3 in Hg removal:

Figures 5.11 and 5.12 show Hg adsorption efficiency as a function of temperature for residence time of 1 and 2 sec. The adsorption efficiencies were slightly lower than those with TiO_2 . All the Hg adsorption efficiencies fell into a 2 to 6% range. The presence of O_2 did not enhance the Hg oxidation, allowing it to form HgO . Adsorption efficiency was observed to be independent of temperature, gas composition, and residence time.

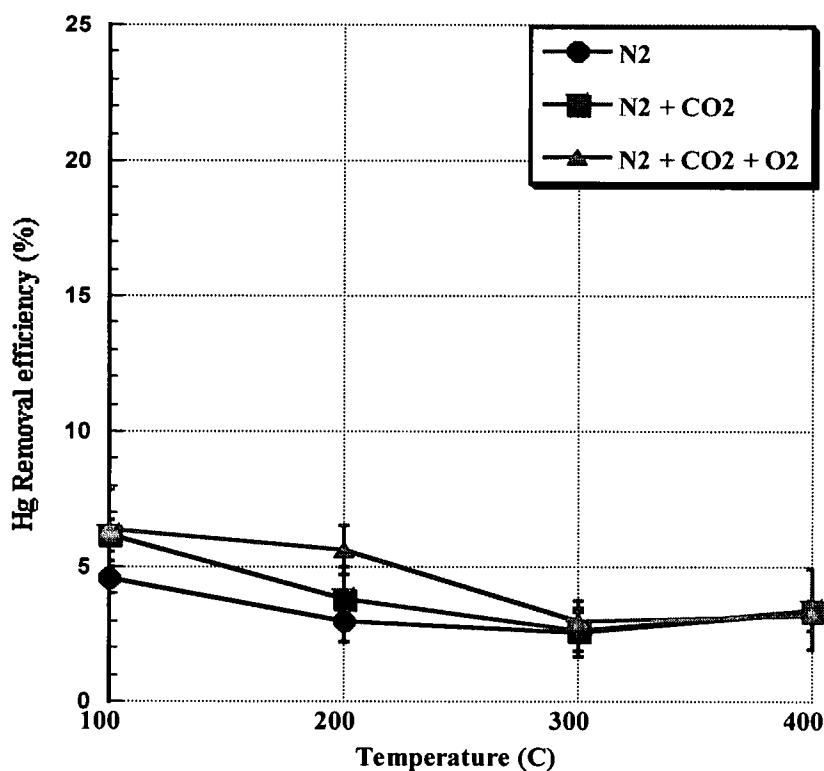


Figure 5.11: Hg removal efficiency as a function of temperature with 0.560 g of Al_2O_3 : R.T. = 1 sec

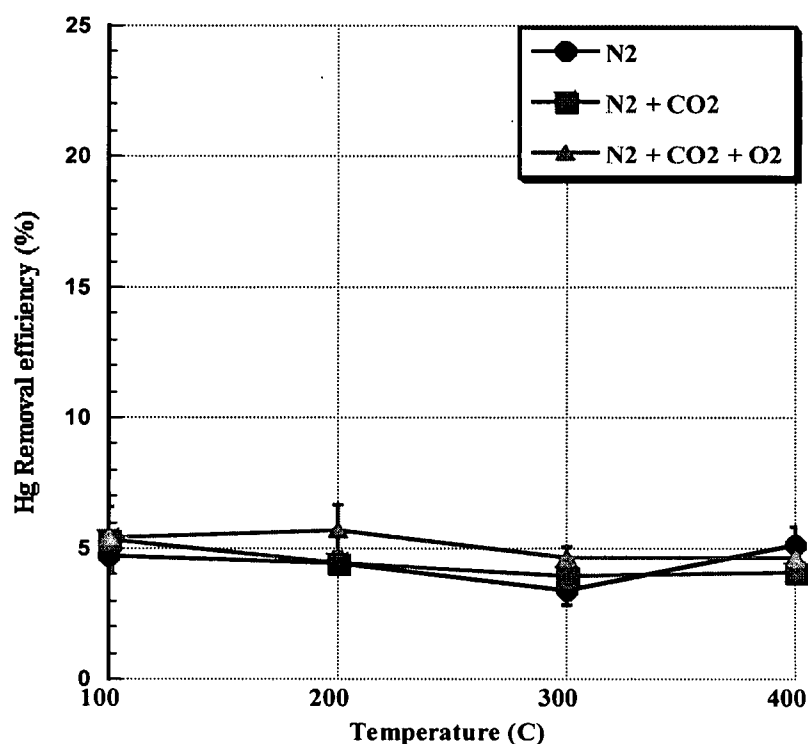


Figure 5.12: Hg removal efficiency as a function of temperature with 0.560 g Al_2O_3 , R.T. = 2 sec

Figures 5.13 and 5.14 show overall Hg removal efficiency with 1 ppm Cl_2 injection at 1 and 2 sec residence time. The results did not show significant temperature dependency. The entire Hg removal efficiency fell into a 5 to 15% range.

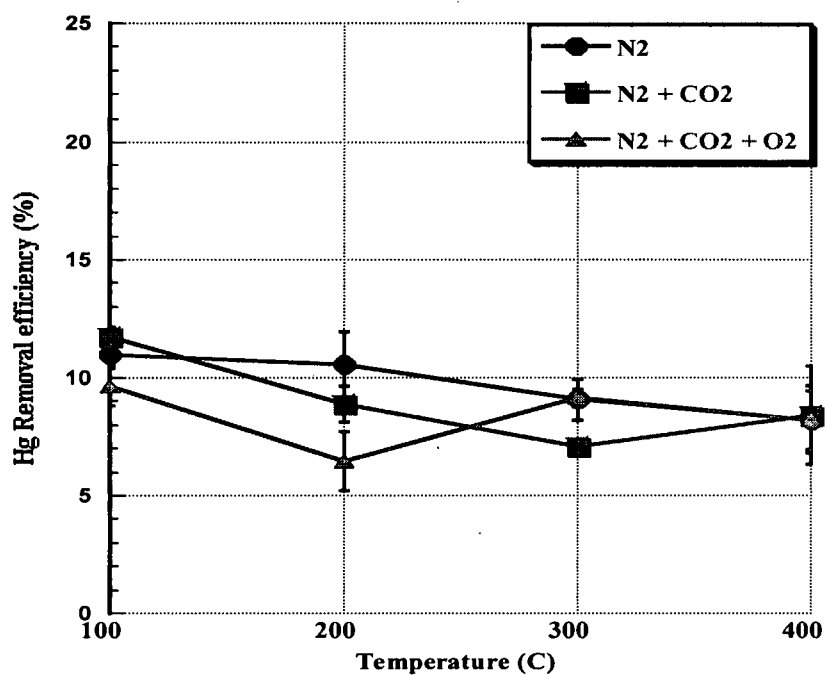


Figure 5.13: Overall Hg removal efficiency as a function of temperature after 1 ppm Cl₂ injection with 0.560 g of Al₂O₃, R.T. = 1 sec

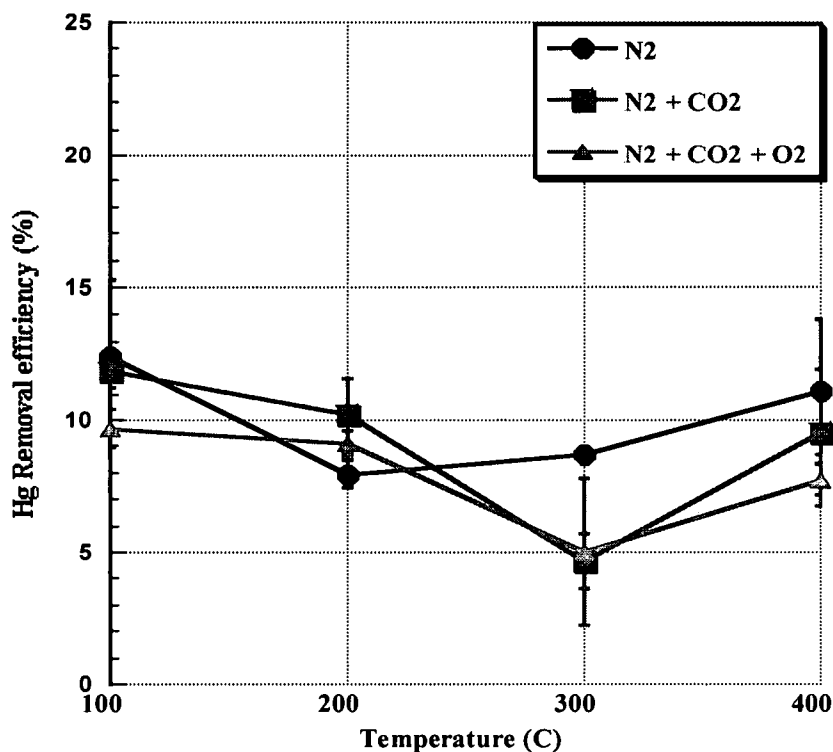


Figure 5.14: Overall Hg removal efficiency as a function of temperature after 1 ppm Cl₂ injection with 0.560 g of Al₂O₃, R.T. = 2 sec

Figures 5.15 and 5.16 show overall Hg removal efficiency with 100 ppm HCl injection at 1 and 2 sec residence time. No distinguishable dependence was observed for the overall Hg removal efficiency with changing gas composition. A slight positive temperature and dependence was observed at the 2 sec residence time compared to the 1 sec residence time.

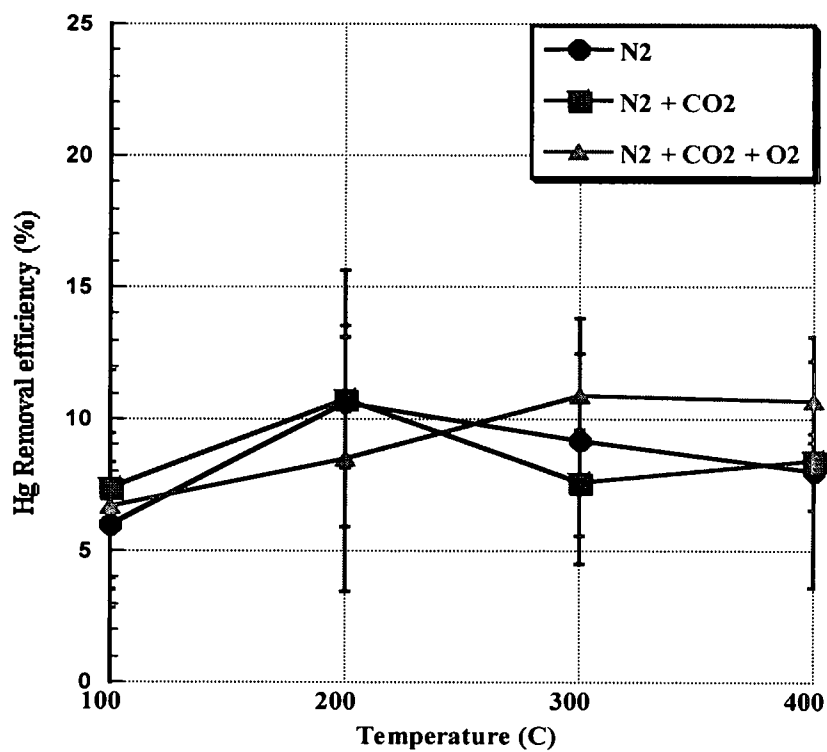


Figure 5.15: Overall Hg removal efficiency as a function of temperature after 100 ppm HCl injection with 0.560 g of Al₂O₃, R.T. = 1 sec

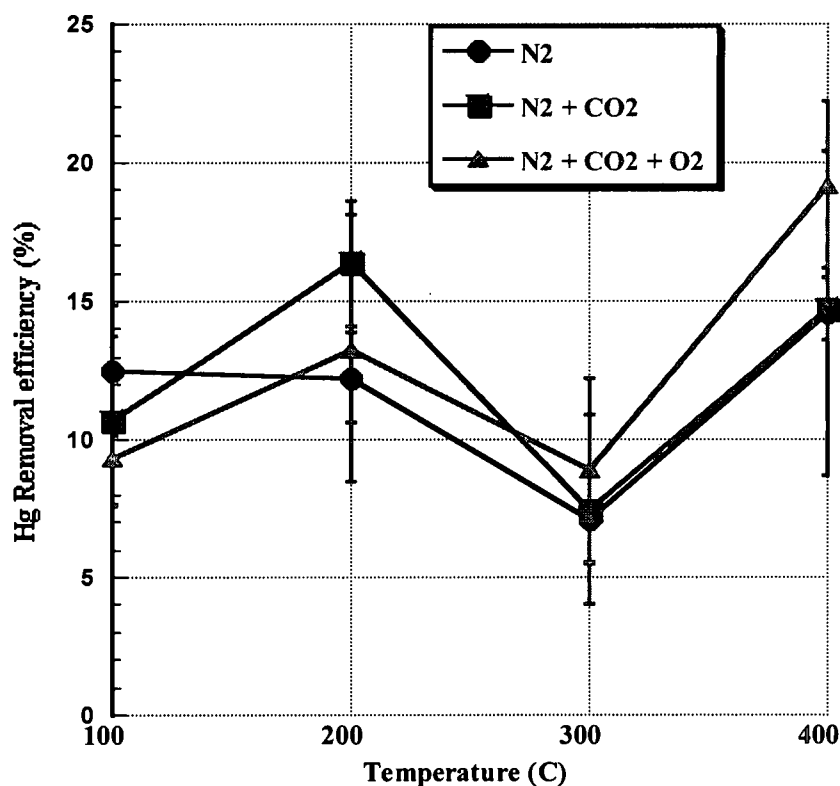


Figure 5.16: Overall Hg removal efficiency as a function of temperature after 100 ppm HCl injection with 0.560 g Al₂O₃, R.T. = 2 sec

Al₂O₃ surface is ineffective for Hg adsorption and oxidation reactions. Al₂O₃ is less effective than TiO₂ for Hg removal. One reason could be its smaller specific surface area, which is approximately one-third titanium dioxide (as shown in Table 4.4). Compared to gas phase oxidation results, the adsorption and oxidation results for Al₂O₃ are the same as the gas phase results, which indicate that Al₂O₃ surface activity in oxidation is minimal. Zhuang indicated that Al₂O₃ was ineffective in capturing mercury¹⁵; our results for Al₂O₃ were comparable with Zhuang's results. Ghorishi also showed that Al₂O₃ is inactive²³; they performed experiments in the presence of HCl in which Al₂O₃ was

ineffective in Hg transformation. Galbreath performed separate measurements of mercury speciation in oxygen and then in nitrogen by injecting $10 \mu\text{g}/\text{m}^3$ of elemental mercury in the presence of two catalysts - Al_2O_3 and TiO_2 . Results showed that the two catalysts were inactive in the transformation of Hg^0 to Hg^{2+} .³²

Effect of CaO in Hg removal:

Figures 5.17 and 5.18 show Hg adsorption data at 1 and 2 sec residence times and temperatures between 100 and 400°C. Adsorption efficiency was observed to be independent of temperature, gas composition, and residence time. All adsorption efficiencies fall into the 3 to 5% range.

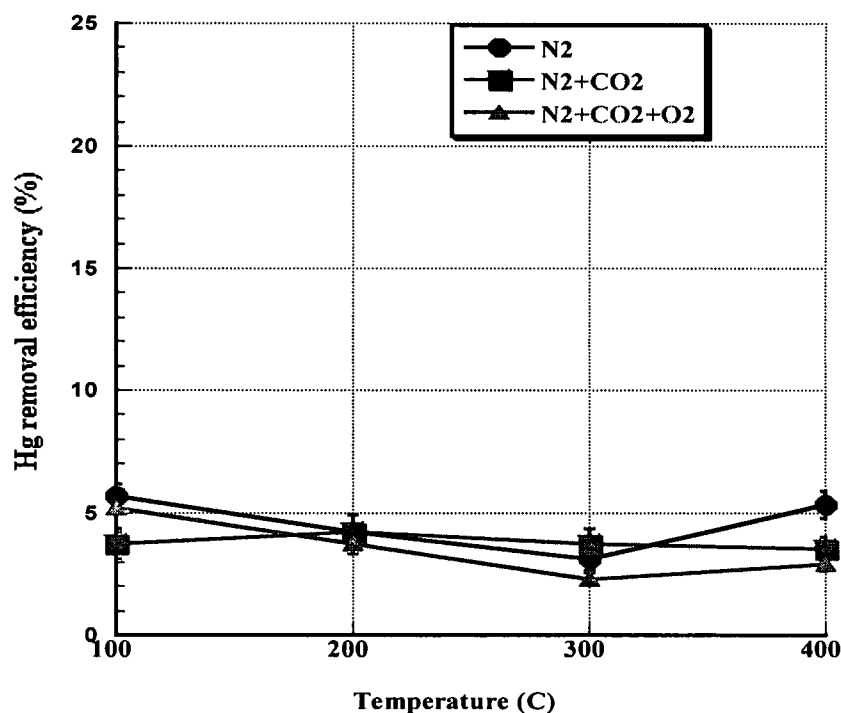


Figure 5.17: Hg removal efficiency as a function of temperature with 0.5374 g of CaO, R.T. = 1 sec

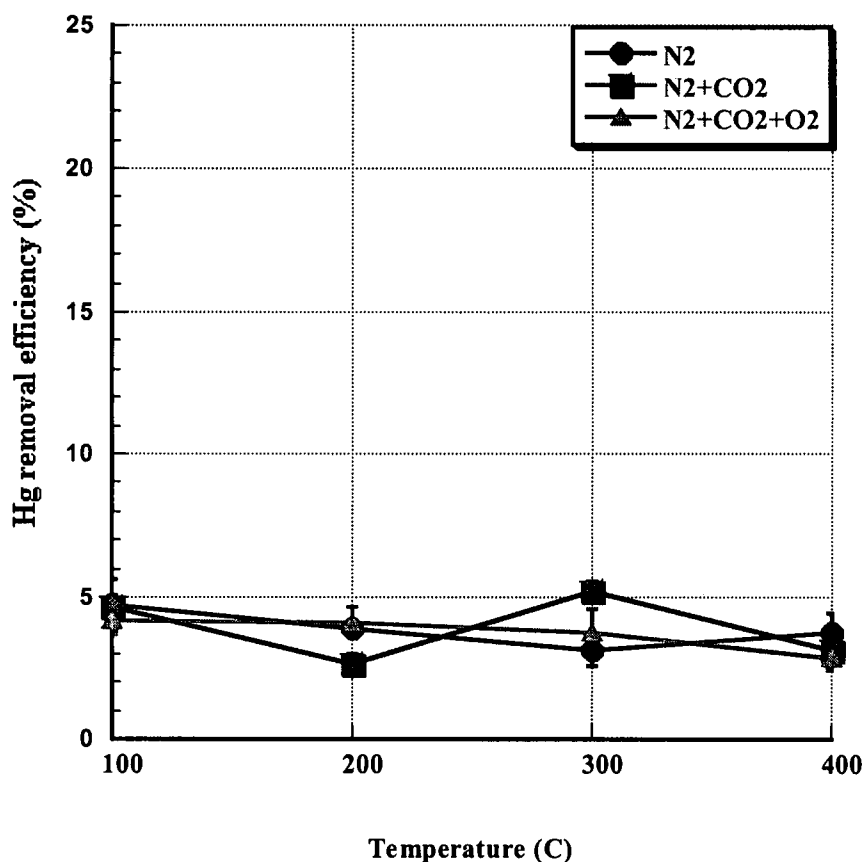


Figure 5.18: Hg removal efficiency as a function of temperature with 0.5374 g of CaO, R.T. = 2 sec

Figures 5.19 and 5.20 show overall Hg removal efficiency with 1 ppm Cl_2 injection at 1 and 2 sec residence time, respectively. The results indicated no significant temperature dependence. No difference was found between adsorption and oxidation results for 1 sec residence time, which signifies that no oxidation has occurred in the presence of CaO surface. High Hg removal efficiency was observed with $\text{N}_2 + \text{CO}_2$ at 100°C and 2 sec residence time compared to other gas compositions (N_2 and $\text{N}_2 + \text{CO}_2 + \text{O}_2$). Under these conditions, experiments were performed six times to check the consistency of the results with $\text{N}_2 + \text{CO}_2$. Results were consistent with a $\pm 3.5\%$ standard deviation.

The reason for the change in Hg removal is not understood because N_2 and CO_2 are inert gases.

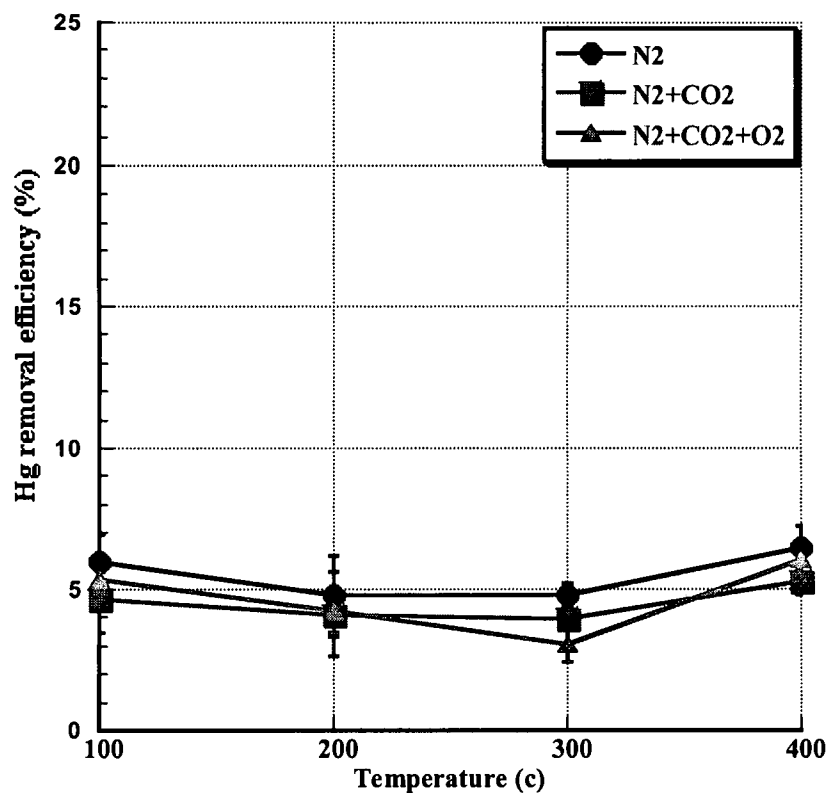


Figure 5.19: Overall Hg removal efficiency as a function of temperature after 1 ppm Cl_2 injection with 0.5374 g CaO, R.T. = 1 sec

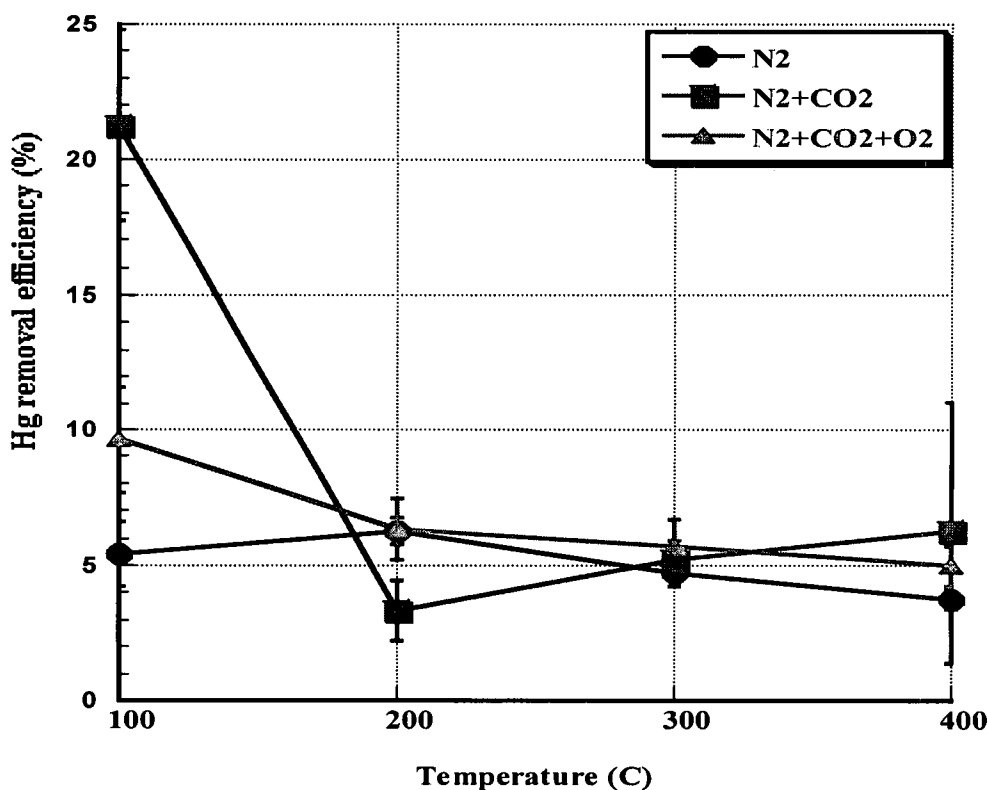


Figure 5.20: Overall Hg removal efficiency as a function of temperature after 1 ppm Cl₂ injection with 0.5374 g of CaO, R.T. = 2 sec

Overall removal efficiencies in the presence of 100 ppm HCl are shown in Figures 5.21 and 5.22. The results indicate no temperature dependence and overall removal efficiencies fall in the 3 to 10% range. The CaO surface is not a reactive site for Hg adsorption and oxidation reactions. CaO results showed inactivity and less adsorption and overall oxidation compared to TiO₂ and Al₂O₃. The presence of Cl₂, O₂, and HCl did not change the reactivity of the CaO surface. Compared to gas-phase and CaO surface results (no chlorine source, adsorption only), CaO Hg removal efficiencies were observed to be lower. The

reason could be that the CaO might act as reducing agent, reducing oxidized Hg to elemental Hg.

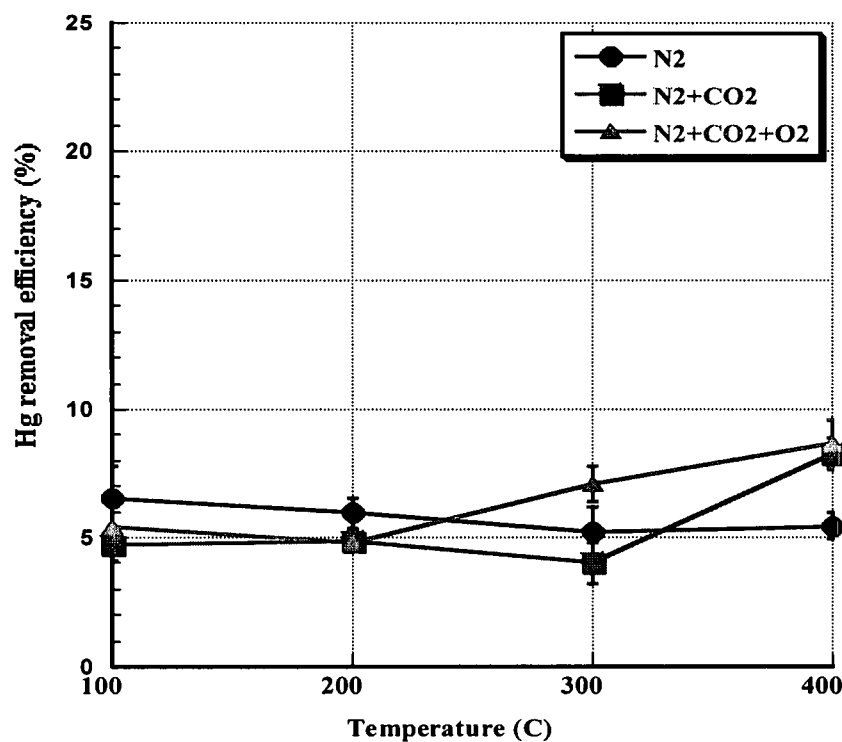


Figure 5.21: Overall Hg removal efficiency as a function of temperature after 100 ppm HCl injection with 0.5374 g of CaO, R.T. = 1 sec

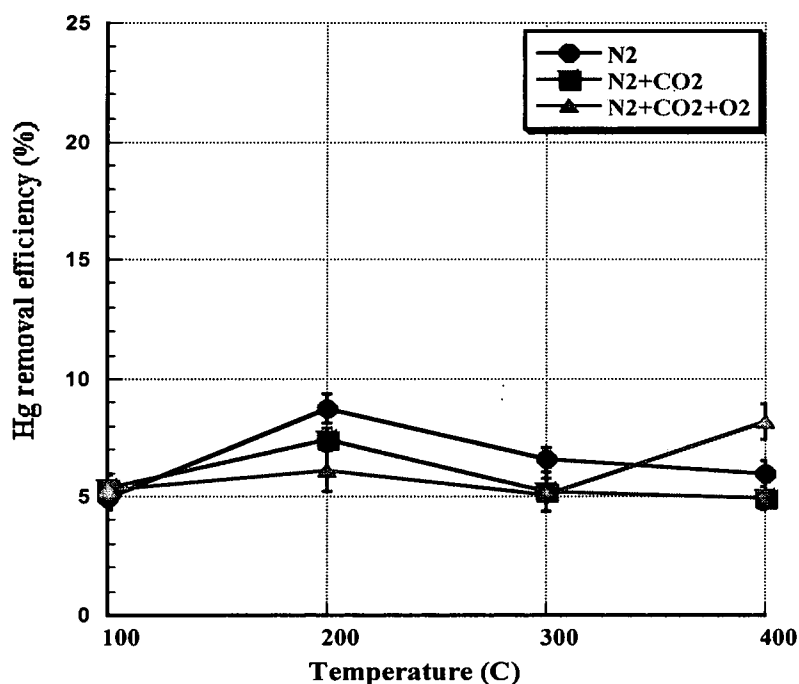


Figure 5.22: Overall Hg removal efficiency as a function of temperature after 100 ppm HCl injection with 0.5374 g of CaO, R.T. = 2 sec

Results for CaO were ineffective for mercury transformations in the presence of HCl and Cl₂. This finding is similar to studies reported by Zhuang where, in the presence of HCl, CaO was inactive in adsorbing mercury.¹⁵ Hocquel conducted laboratory-scale experiments to determine the effect of CaO on Hg speciation. The experiments were conducted in the presence of HCl and resulted in the conversion of HgCl₂ (g) to elemental mercury at temperatures above 27°C (300 K). Forty to fifty percent of HgCl₂ was converted to elemental mercury at 177°C (450 K).²⁹ Hocquel's results are consistent with the CaO results presented here.

Effect of $\gamma\text{-Fe}_2\text{O}_3$ in Hg removal:

Figures 5.23 and 5.24 show Hg adsorption efficiencies at residence times of 1 and 2 sec. At 200°C, 1 sec and 300°C, 2 sec, adsorption efficiencies were slightly higher when O₂ was included with the carrier flow. This result indicates that Hg was oxidized with O₂ on the iron oxide surface. Adsorption efficiencies are calculated based on the difference in elemental Hg concentration between the front and back end of the reactor. An Hg analyzer can only detect elemental Hg, it cannot differentiate between elemental and oxidized Hg. Therefore, the increase in Hg removal efficiency in the presence of oxygen compared to N₂ and N₂+CO₂ was attributed to Hg oxidation by O₂ to form HgO. Adsorption efficiency did not show a positive temperature dependency. Compared to the other metal oxides studied, $\gamma\text{-Fe}_2\text{O}_3$ exhibited a higher adsorption efficiency.

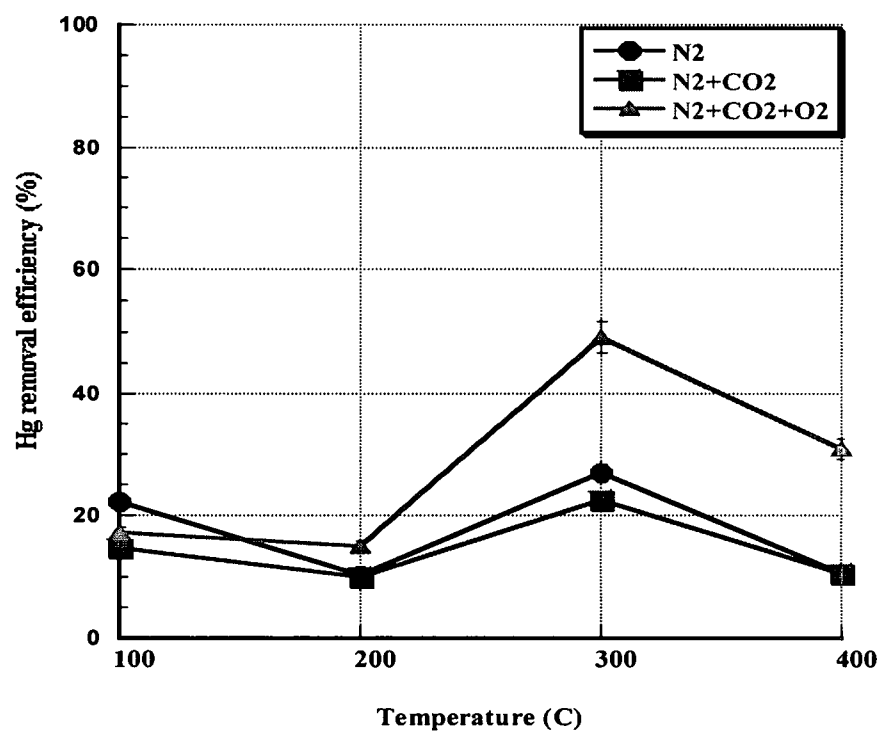


Figure 5.23: Hg removal efficiency as a function of temperature with 0.564 g of Fe₂O₃, R.T. = 1 sec

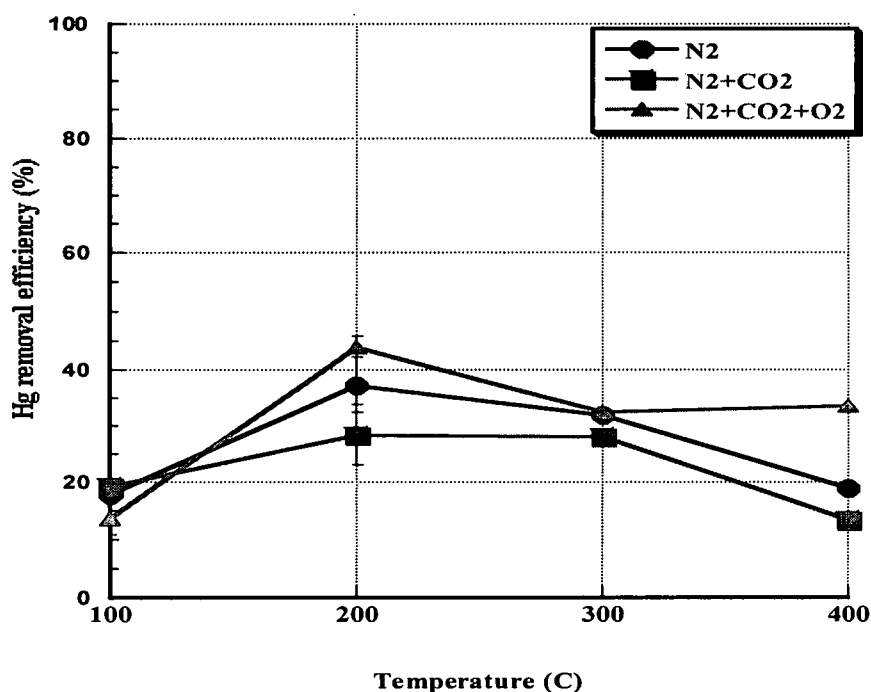


Figure 5.24: Hg removal efficiency as a function of temperature with 0.564 g of Fe_2O_3 , R.T. = 2 sec

Figures 5.25 and 5.26 represent overall Hg removal efficiencies when 1 ppm Cl_2 was injected. Significant difficulties were encountered in obtaining consistent results for this surface. At 1 sec residence time, the results showed a relatively high Hg removal efficiency at 200°C and below. At 300°C, the Hg removal efficiency dropped drastically to a level below the adsorption efficiency (as shown in Figure 5.25). The reason for this phenomenon is not clearly understood; however, a possible explanation could be catalyst aging and complex Hg adsorption/desorption and oxidation/reduction behavior on the Fe_2O_3 surface. The iron oxide surface was exposed to Hg throughout the experiments and Hg might be strongly bonded on the surface causing it to become saturated.

The surface was purged every time the experimental condition was changed, but the impact of the Hg interaction may have been irreversible.

At 300°C gas composition, $\text{N}_2 + \text{CO}_2 + \text{O}_2$ showed a high Hg removal efficiency compared to other gas compositions (N_2 , $\text{N}_2 + \text{CO}_2$). The reason could be the presence of O_2 which might have played an important role in oxidizing Hg. At 400°C, the Hg removal efficiency was over 90%.

Similar apparent experimental inconsistency was also observed for the 2 sec experiments. These results cannot be easily described and require further investigation. Surface analysis of aged iron oxide powder would be helpful in understanding the results. Hg removal efficiency study as a function of aging would also be helpful.

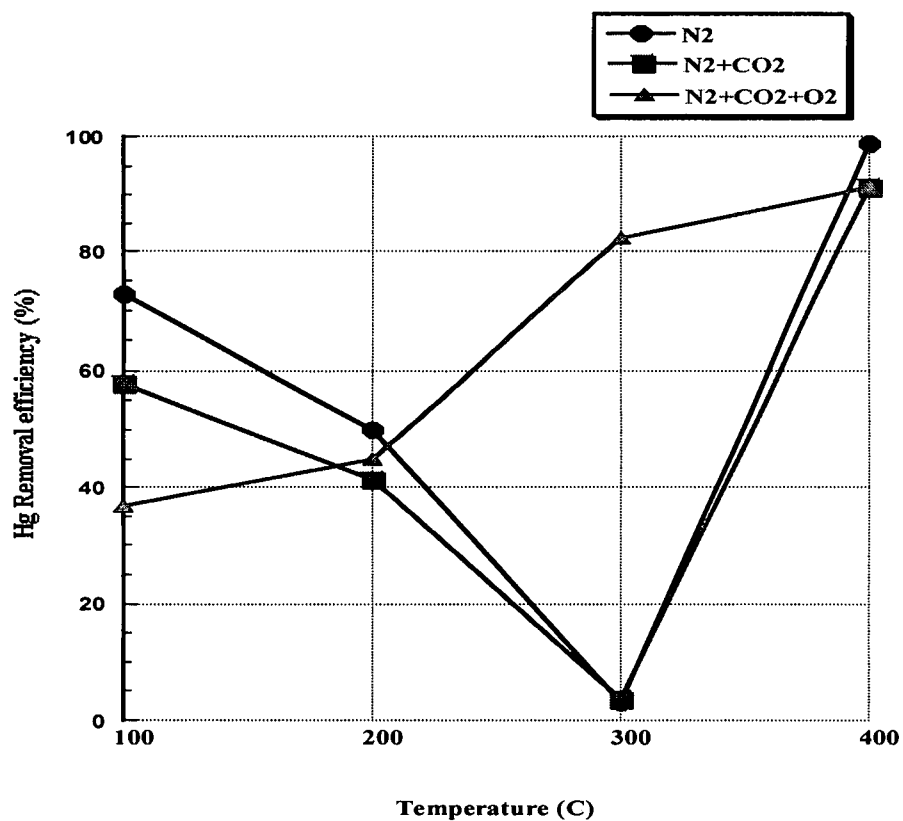


Figure 5.25: Overall Hg removal efficiency as function of temperature after 1 ppm Cl₂ injection with 0.564 g Fe₂O₃, R.T. = 1 sec

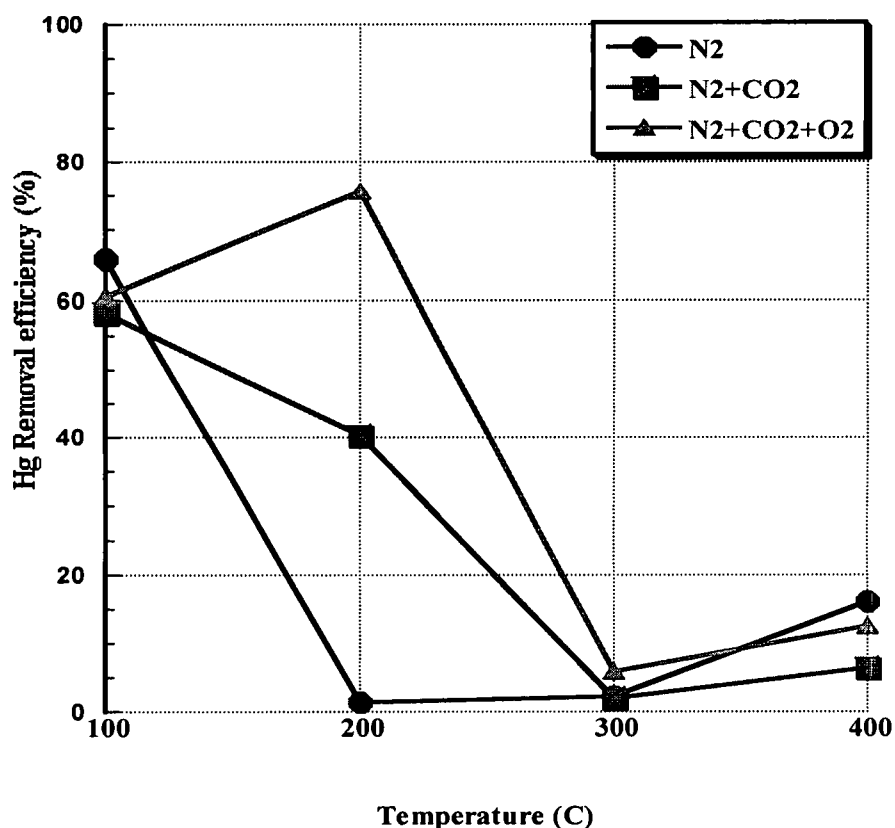


Figure 5.26: Overall Hg removal efficiency as a function of temperature after 1 ppm Cl₂ injection with 0.564 g Fe₂O₃, R.T. = 2 sec

Figures 5.27 and 5.28 represent overall Hg removal efficiency following the injection of 100 ppm of HCl. At 1 sec residence time, iron oxide showed higher removal efficiency than other metal surfaces. In general, iron oxide exhibited positive and negative temperature dependence at 1 and 2 sec, respectively. Further study is necessary to more fully understand how iron oxide functions as an oxidation and reduction agent, depending on the residence time.

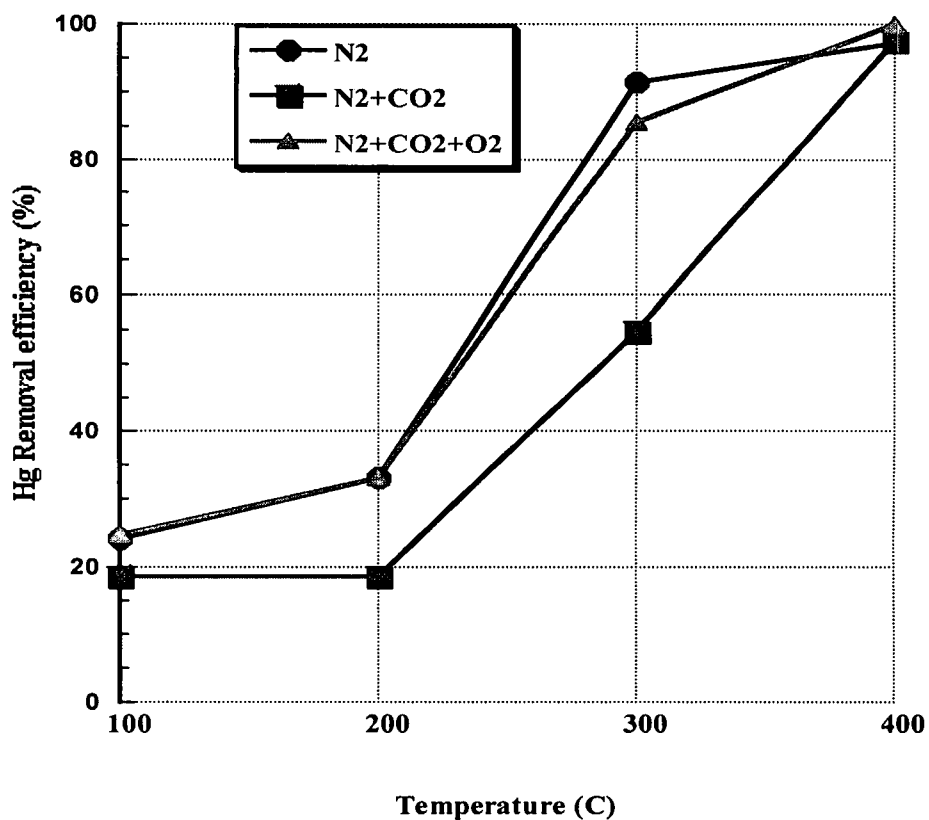


Figure 5.27: Overall Hg removal efficiency as a function of temperature after 100 ppm HCl injection with 0.564 g Fe₂O₃, R.T. = 1 sec.

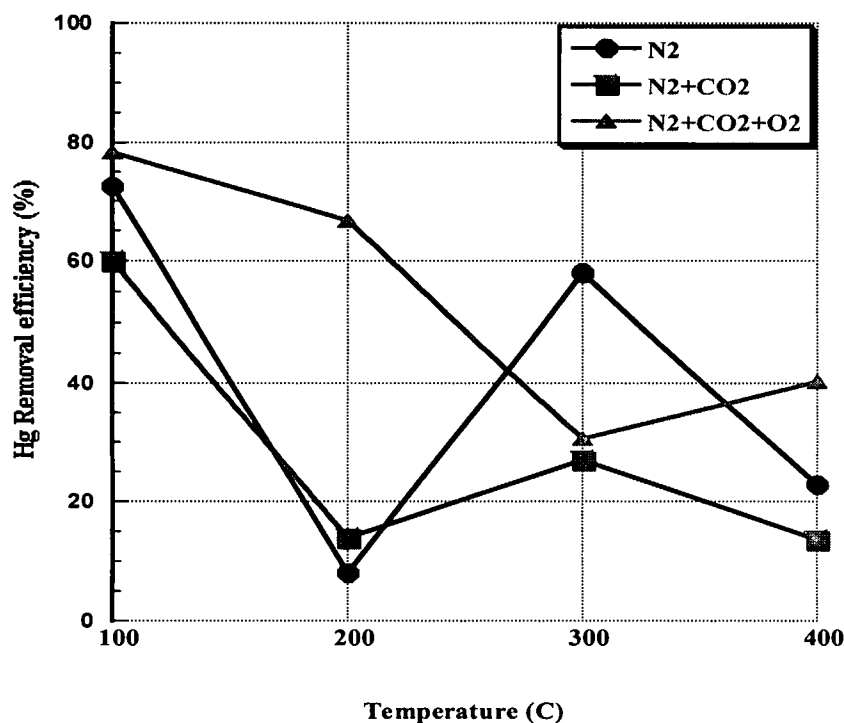


Figure 5.28: Overall Hg removal efficiency as a function of temperature after 100 ppm HCl injection with 0.564 g Fe₂O₃, R.T. = 2 sec

Investigations by Wu demonstrated that in the presence of HCl, iron oxide suppressed the elemental mercury removal efficiency. The concentration of HCl maintained in the reaction was 1 ppm, and it was observed that a constant removal level of elemental Hg was obtained after 3 hours.³³ Ghorishi reported that γ -Fe₂O₃ promotes Hg oxidation, especially in the presence of HCl. The tests suggested that γ -Fe₂O₃ was a good oxidizing agent and can transform Hg⁰ to Hg²⁺ in the presence of 100 ppm of HCl. Approximately 30% of Hg⁰ was transformed to Hg²⁺ and/or Hg(p) at 150°C.²⁶ Wu concluded that the sorbents which contained iron oxide can effectively capture mercury at temperatures from 60-100°C, and that the effective removal increased with increases in

temperature.³⁴ The results of this investigation at 1 sec residence times in the presence of Cl_2 and HCl sources showed a higher overall Hg removal efficiency, which is comparable to Wu's results. Wu examined Hg removal efficiencies in the presence of Fe_2O_3 nanoparticles in the 180-320°C temperature range and proposed that in the presence of air, Fe_2O_3 nanoparticles are adsorbed or desorbed.³⁵ Ghorishi also demonstrated that Fe_2O_3 exhibited significant catalytic activity in the surface-related oxidation of Hg^0 .²³

Figures 5.29 through 5.32 show a comparison of gas phase, adsorption, and overall Hg removal efficiency for all catalysts at residence times of 1 and 2 sec in the presence of Cl_2 and or HCl , and N_2 . From Figures 5.29 and 5.30, it was observed that for $\gamma\text{-Fe}_2\text{O}_3$ and TiO_2 , overall Hg removal efficiency was higher compared to gas phase and other catalysts (CaO and Al_2O_3) with Cl_2 injection. From Figures 5.31 and 5.32 with presence of HCl , the overall removal efficiency for $\gamma\text{-Fe}_2\text{O}_3$ and TiO_2 was higher and also adsorption for $\gamma\text{-Fe}_2\text{O}_3$ was higher than gas phase oxidation and other catalysts (CaO and Al_2O_3). Compared to gas phase results, the $\gamma\text{-Fe}_2\text{O}_3$ and TiO_2 showed surface oxidation. Although Al_2O_3 showed slightly higher overall Hg removal than adsorption efficiencies, the overall Hg removal efficiency is similar to gas phase oxidation. CaO was ineffective for the Hg transformation in presence of HCl and Cl_2 . When compared to gas phase results, CaO did not show significant surface oxidation, which shows its ineffectiveness and played a major role as reducing agent.

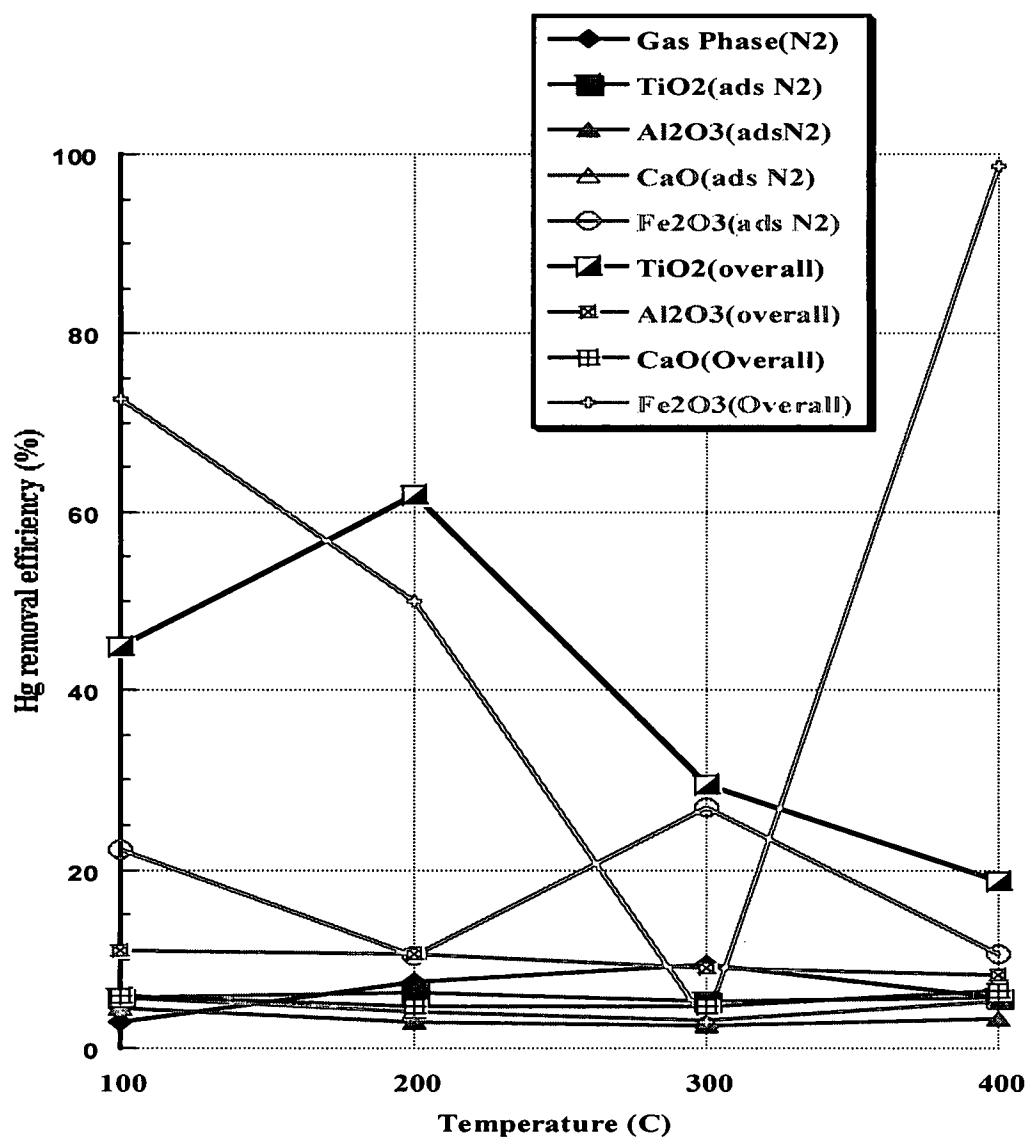


Figure 5.29: Hg removal efficiency as a function of temperature after 1 ppm Cl_2 injection in presence of N_2 gas with combination of all catalysts and gas phase, R.T. = 1 sec

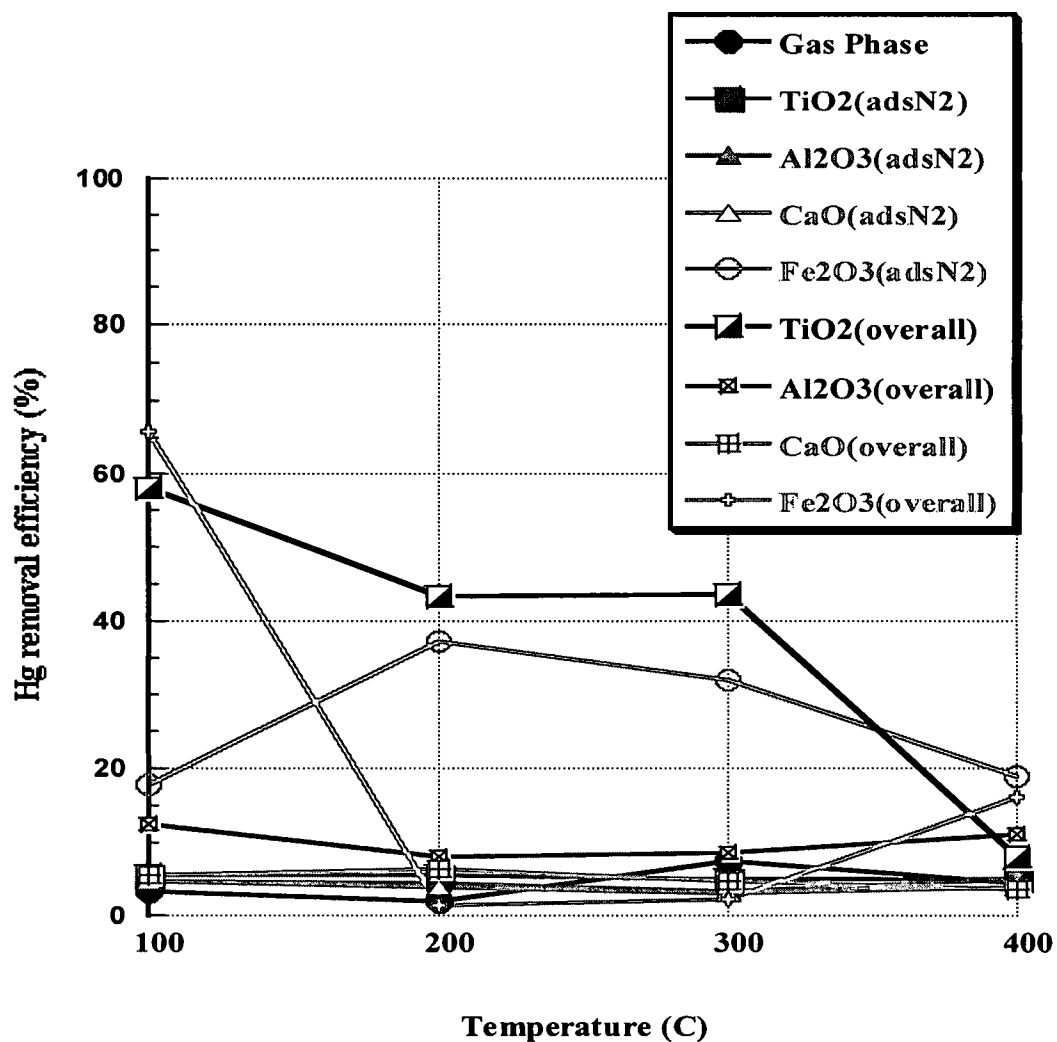


Figure 5.30: Hg removal efficiency as function of temperature after 1 ppm Cl_2 injection in presence of N_2 gas with combination of all catalysts and gas phase, R.T. 2 sec

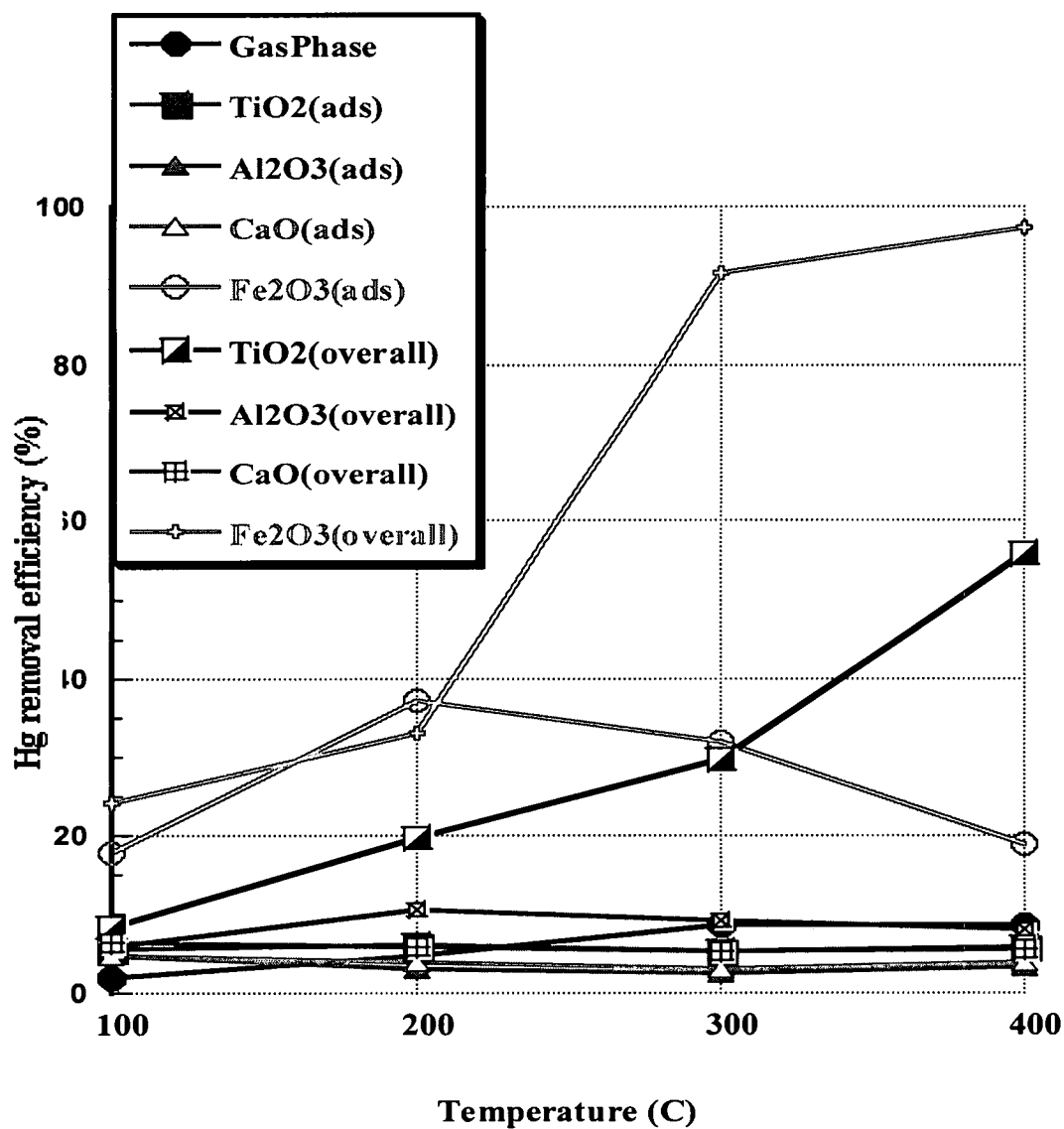


Figure 5.31: Hg removal efficiency as function of temperature after 100 ppm HCl injection in presence of N₂ gas with combination of all catalysts and gas phase, R.T. = 1 sec

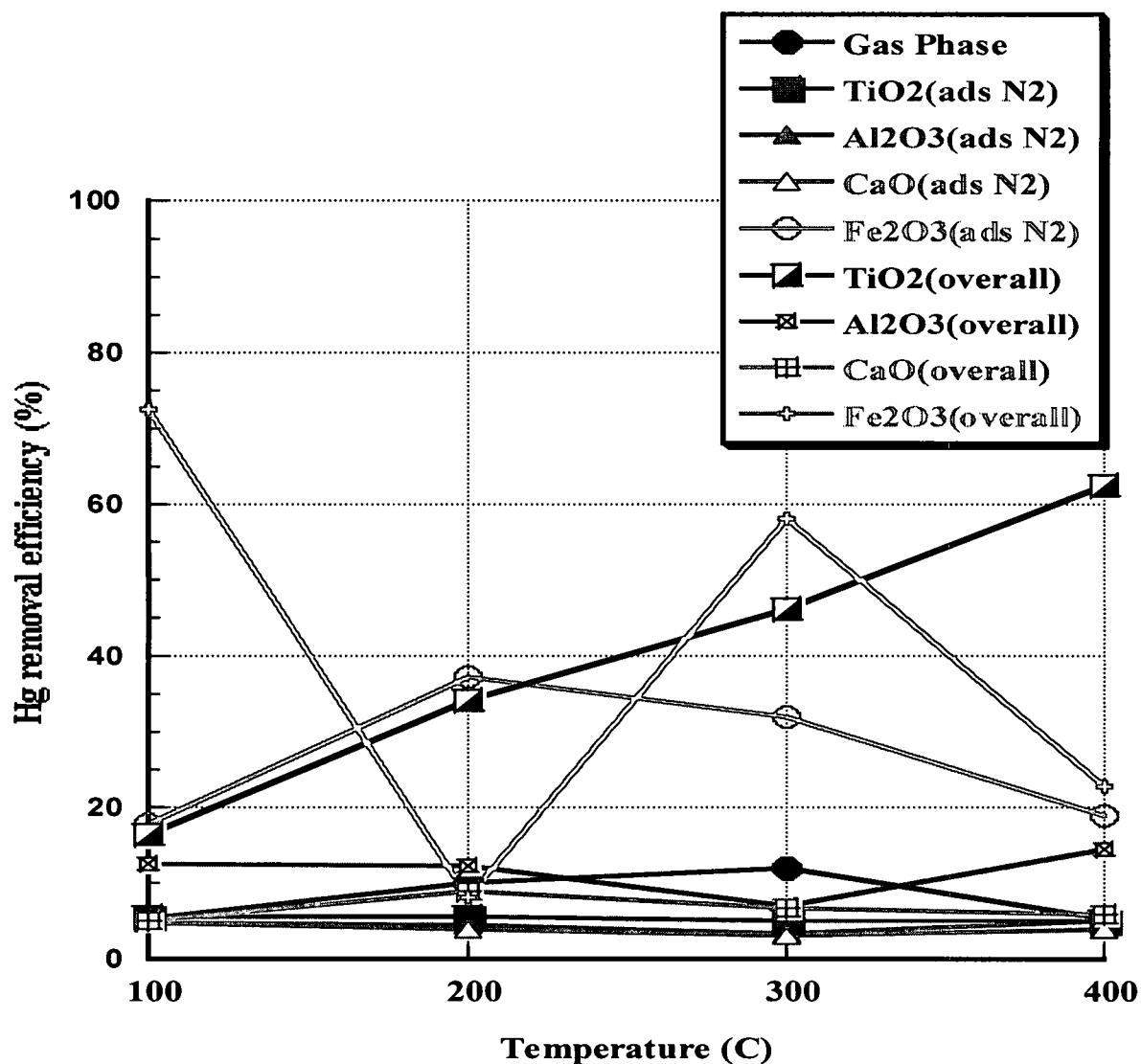


Figure 5.32: Hg removal efficiency as function of temperature after 100 ppm HCl injection in presence of N₂ gas with combination of all catalysts and gas phase: Residence time 2 sec

CHAPTER VI

CONCLUSIONS

Experiments were designed to investigate Hg transformation under homogeneous (gas-phase) and heterogeneous (gas-surface) environments in presence of chlorine sources (Cl_2 and HCl). The following conclusions were drawn from the experimental studies:

- Gas phase results did not show any measurable difference for Hg oxidation at 1 and 2 sec residence time, for the various gas compositions in the presence of either HCl or Cl_2 .
- Surface activity of catalysts, in terms of adsorption only, followed the following descending order of reactivity: $\text{Fe}_2\text{O}_3 > \text{TiO}_2 > \text{Al}_2\text{O}_3 > \text{CaO}$. The overall Hg removal efficiency in the presence of Cl_2 or HCl followed the same descending order of reactivity.

For iron oxide, the data was highly scattered and further investigation is needed to elucidate the Hg adsorption and oxidation mechanisms. TiO_2 , in presence of Cl_2 , showed high overall Hg removal efficiencies at low temperatures. TiO_2 , in presence of HCl , showed high overall Hg removal at high temperature (400°C).

CHAPTER VII

RECOMMENDATIONS FOR FUTURE WORK

Recommendations for additional study of Hg transformation reactions in the presence of metal oxide surfaces are given below:

- To produce more repeatable results, it would be desirable to use a new reactor for each experiment.
- Heterogeneous studies need further investigation; e.g., surface analysis studies for $\gamma\text{-Fe}_2\text{O}_3$. Aging of catalyst is considered to be a reason for loss of surface activity for this metal oxide.
- Study of actual fly ashes is necessary to fully understand Hg transformation.
- Elucidating the mechanism of the surface chemistry involved during the adsorption and overall Hg removal would be a major advance in designing an effective technology for Hg removal in full-scale systems.

CHAPTER VIII

REFERENCES

1. Othermer, K. Encyclopedia of Chemical Technology. (2006), Ed. 5, Vol. 16.
2. Hill, F. C., Laboratory of Physics, Univ. of Illinois, Phys. Rev. (1922), 20, 259-266.
3. *Characterization of products containing mercury in municipal solid waste in the United States, 1970-2000*, OSW No.EPA530-R-92-013 (NTIS no.PB92-162 569), U. S. Environmental Protection Agency.
4. *Global Mercury Assessment*
(www.chem.unep.ch/Mercury/Report/Key-findings.htm).
5. United States Department of Labor, Occupational Safety and Health Administration
(<http://www.osha.gov/SLTC/healthguidelines/mercuryvapor/recognition.html>)
6. *Mercury Study Report to Congress*, December (1997), Volume 1, EPA-452/R-97-003.
7. *Controlling Power Plant Emissions*, US-EPA Report
(http://epa.gov/mercury/control_emissions/emissions.htm).
8. *Chemical and Engineering News*, March 2, page 13, 2009
(WWW.CEN-ONLINE.ORG).
9. Dunham, G.E., Dewall, R.A. and Senior, C.L., Fuel Process. Technol. (2003), 82,197-213.
10. Niksa, S. and Fujiwara, N. (2004) *Predicting Complete Hg Speciation Along Coal-fired Utility Exhaust Systems*, Combined Power Plant Air Pollution Control Mega Symposium, Washington, D.C.
11. Pavlish, J.H., Sondreal, E.A., Mann, M.D., Olson, E.S., Galbreath, K.C., Laudal, D.L., and Benson, S.A., Fuel Process. Technol. (2003), 82, 89-165.

12. Sondreal, E.A., Benson, S.A., Pavlish, J.H., Ralston, N.V.C., Fuel Process. Technol. (2004), 85, 425-440.
13. *Mercury Speciation and Capture* (www.lpetag.org/600R01109chap5.pdf).
14. Sakulpitakphon, T., Hower, J.C., Trimble, A.S., Schram, W.H. and Thomas, G.A., Energ. Fuel (2000), 14, 727-733.
15. Zhuang Y., Thompson J. S., Zygarlicke C.J. and Pavalish J.H., Environ. Sci. Technol. (2004), 38, 5803-5808.
16. Niksa, S. and Fujiwara, N. *Predicting the Levels and Speciation of Mercury in Coal-derived Utility Exhaust Streams*, Proceedings of the 28th International Technical Conference on Coal Utilization and Fuel Systems, (2003), 199-210.
17. Galbreath, K.C. and Zygarlicke, C.J., Environ. Sci. & Technol. (1996), 30, 2421-2426.
18. Serre, D.S., Silcox, G.D., Ind. Eng. Chem. Res. (2000), 39, 1723-1730.
19. Senior, C., Modeling Gaseous Mercury Behavior in Practical Combustion Systems. In Proceedings of the Air Quality III: Mercury, Trace Elements, and Particulate Matter Conference; Arlington, VA, (2002), Sept 10-12.
20. Niksa, S. and Fujiwara, N., *Predicting Mercury Speciation in Coal-Derived Flue Gases*, Paper No. 69190.
21. Hall B., Schager P., and Lindqvist O., Water, Air, Soil Pollution (1991), 56, 3-14.
22. Kramlich, J.C., Sliger, R.N. and Marinov, N.M., Fuel Process. Technol. (2000), 65-66, 423-438.
23. Ghorishi, S.B., Lee, C.W., Jozewicz, W.S. and Kilgroe, J D., Environ. Eng. Sci., (2005), 22:221-231.
24. Norton, G. A., Yang, H., Brown, R C., Laudal, D. L., Dunham, G.E., and Erjavec, J., Fuel Process. Technol. (2003), 82, 107-116.
25. Galbreath, K.C. and Zygarlicke, C.J., Fuel Process. Technol. (2000), 65-66, 289-310.
26. Ghorishi, S.B., Lee, C.W., and Kilgroe, J.D. Air & Waste Management Association 92nd Annual Meeting & Exhibition, St. Louis, MO, June 20-24 (1999); Paper 99-651.

27. Galbreath, K.C., Zygarlicke, C.J., Tibbetts, J.E., Schulz, R.L. and Dunham, G.E., *Fuel Process. Technol.* (2005), 86, 429-448.
28. Zhuang, Y., Thompson J.S., Zygarlicke, C.J., Pavlish, J.H., *Fuel Process. Technol.* (2007).
29. Hocquel, M., Unterberger, S. and Hein, K.R.G., *Chem. Eng. Technol.* (2001), 24, 12.
30. Brahman, R.K. *Gas Phase and Surface Kinetics of Mercury Chlorination*, M. S. Thesis, University of Dayton, Department of Chem. Eng. (2006).
31. Poindexter, F.E., *Mercury Vapor Pressure at Low Temperatures*, 859-868.
32. Galbreath, K.C., Zygarlicke, C.J., Olson, E.S., Pavlish, J.H. and Toman, D.L., *Science Total Environ.* (2000), 261, 149-155.
33. Wu, S., Ozaki M., Azhar, Md. and Sasaoka, E., *Fuel* (2008), 87, 467-474.
34. Wu, C., Md, Azhar and Sasaoka, E., *Fuel* (2006), 85, 213-218.
35. Wu, C.Y., Borderieux, S., Bonzongo, J.C., and Powers, K., *Aerosol and Air Quality Research* (2004), 4, 74-90.
36. Ghorishi, S.B. and Gullett, B.K., 1997, EPRI-DOE-EPS Combined Utility Air Pollutant Control Symposium, Washington, DC.

R002594315